AD-A042 392 RENSSELAER POLYTECHNIC INST TROY N Y DEPT OF MATERIA--ETC F/G 11/6
HIGH TEMPERATURE EUTECTIC COMPOSITES: MECHANICAL BEHAVIOR.(U)
JUL 77 N S STOLOFF N00014-75-C-0503
UNCLASSIFIED TR-3 NL

| OF |
ADA042392

END
DATE FILMED
8-77
DDC

Technical Report No. 3
to
Office of Naval Research
Contract N00014-75-C-0503, NR 031-745

entitled

HIGH TEMPERATURE EUTECTIC COMPOSITES: MECHANICAL BEHAVIOR

Submitted by

N. S. Stoloff
Rensselaer Polytechnic Institute
Troy, New York 12181, USA

July 15, 1977

Technical Report No. 3
to
Office of Naval Research
Contract N00014-75-C-0503, NR 031-745

entitled

HIGH TEMPERATURE EUTECTIC COMPOSITES: MECHANICAL BEHAVIOR

Submitted by

N. S. Stoloff
Rensselaer Polytechnic Institute
Troy, New York 12181, USA

July 15, 1977

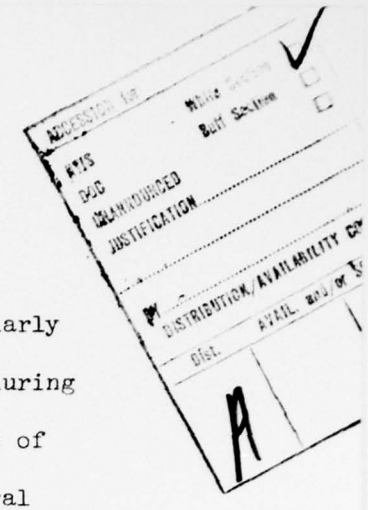

I. Introduction

The mechanical behavior of eutectic composites, particularly at elevated temperatures, has received considerable attention during the past decade. This is a consequence of early demonstrations of superior tensile, creep, and stress rupture properties of several nickel and cobalt-base eutectics. It has been established that further significant increases in static strength and fatigue resistance of many eutectics can be achieved through control of microstructural parameters, particularly interphase spacing, λ, and by inducing precipitation or ordering phenomena through post-solidification heat treatments. Interphase spacing in many alloys can be refined through increasing growth rate, R, so long as the critical ratio of temperature gradient, G, to growth rate, R, for the alloy can be maintained. Work on many systems has confirmed the following relationship between R and λ:

$$\lambda^2 R = \text{constant} \qquad (1)$$

where the constant varies between systems.[1]

Typical microstructures achieved in several nickel and cobalt-base high temperature alloys to be discussed in this paper are shown in Fig. 1. Representative compositions of these and other alloys discussed in this review (which may vary somewhat from one laboratory to another) are summarized in Table 1.

Several nickel-base eutectics containing aluminum, most notably Ni,Al,Cr-TaC (Nitac) and Ni,Nb,Cr,Al (γ/γ'-δ), have been shown to respond to post-solidification heat treatments to precipitate γ' (Ni_3Al). This and other examples of the use of post-solidification heat treatments

will be cited in this review. This paper will also survey in detail, relying upon recently published as well as unpublished data, creep and stress rupture behavior of aligned eutectics, cyclic behavior at both room and elevated temperatures, as well as impact, thermal fatigue and other aspects of mechanical properties of interest to structural designers. Throughout the paper the emphasis will be on understanding mechanisms of plastic flow and thereby controlling microstructures to optimize properties.

II. Tensile Strength

1. Stresses Applied Parallel to Growth Direction

Eutectic alloys have been categorized by Ashbrook[2] according to the plasticity of the coexisting phases: i.e., ductile-ductile (D-D), ductile-semibrittle (D-SB), and ductile-brittle (D-B) (in most eutectics the matrix phase is ductile, but this is not invariably so). This terminology also is observed in Table 2, which summarizes room temperature tensile properties of the alloys listed in Table 1. The strongest of these eutectic alloys exhibit 0.2% offset yield stresses in the range 800-1050 MN/m^2, and ultimate tensile strengths of 1300-1550 MN/m^2. Similar room temperature tensile strength has been reported also for a lamellar Ni,Cr,Al,Fe alloy (fcc γ strengthened by a CsCl type β phase) which has the added advantages of high ductility and density in the range 7.2-7.6 g/cc.[3] Stress strain curves for Nitac and Cotac type alloys demonstrate that appreciable ductility can be attained even when fibers are quite brittle.[4,5] While carbide-reinforced alloys and such new alloys as γ'/γ-Mo are ductile even at 25°C, γ/γ'-δ with 6%Cr

is capable of only 2-4% elongation or reduction in area.[6] However, even γ/γ'-δ can demonstrate appreciable ductility when chromium is removed.[6]

A comparison of tensile strengths of several eutectic alloys with temperature is shown in Fig. 2. Cotac 74, which is, in fact, a nickel-base alloy reinforced by NbC fibers, is the strongest alloy of those shown at room temperature; at 1000°C Nitac 13 exhibits the highest strength, and above 1000°C most of the eutectic alloys shown in Fig. 2 are stronger than conventional superalloys such as IN-100.

The most significant microstructural feature directly related to strength in mechanically combined composite materials is the volume fraction, V_f, of reinforcement. In the case of aligned eutectics V_f is near or below 10% for Cotac, Nitac and other alloys of fibrous microstructure, while γ/γ'-δ and other lamellar alloys normally have larger volume fractions of the non-continuous (reinforcing) phase. Nevertheless, as shown in Fig. 2, some low volume fraction fibrous alloys can be significantly stronger than lamellar eutectics of the same base metal.

The rule of mixtures, which successfully relates tensile strength, σ_c, to volume fraction of the reinforcing phases in mechanically combined composites:

$$\sigma_c = \sigma_f V_f + \sigma_m'(1-V_f) \qquad (2)$$

where σ_f is the tensile strength of the fibers and σ_m' is the stress in the matrix at fracture of fibers, is often incorrectly applied to eutectic composites. Eq. 2 is strictly applicable only to materials deforming with the fibers in the elastic range, while a number of eutectic composites deform readily by plastic deformation of <u>both</u> coexisting phases. Bibring[4]

has reviewed several parameters that can cause deviation from Eq. 1. A difference in Poisson's ratio of the two phases of the eutectic results in high transverse stresses in the composite. Consequently, part of the matrix remains elastic near the interface. This effect increases when the total area of the interface increases, i.e., with decreasing interlamellar spacing. Strengthening may also be due to dislocations interacting with the interface. Cline and Stein[7] have reported that if the interfacial bond is strong enough to resist shear in the two phases, an image force barrier to dislocation motion is set up at the interface. Shaw[8] has shown that a Hall-Petch type of relation exists between the compressive strength of the Cd-Zn eutectic composite, σ_c^*, and the interlamellar spacing, λ:

$$\sigma_c^* = \sigma_i + k\lambda^{-1/2} \tag{3}$$

where σ_c^* is the yield strength of the composites, σ_i the fractional lattice resistance encountered by a glide dislocation as it moves in the matrix, and k the Hall-Petch slope of the curve relating σ to λ. This relation implies that a pile-up of dislocations against lamellae occurs, such that the stress concentration decreases with decreasing values of λ; therefore, the strength of the composite increases. Other workers have demonstrated that Eq. 3 adequately describes the behavior of Ni_3Al-Ni_3Nb (γ'-δ) both at room temperature and at 1093°C,[9] Fig. 3. However, Chadwick[94] has pointed out that some published data could as well be plotted against λ^{-1} or vs. λ with equally good results, and has generally questioned the basis for the widespread use of Eq. 3. Recently Sahoo et al.,[82] in their work on Cd-Zn in tension and compression, noted that the flow stress could be expressed as a

function of solidification rate, R:

$$\sigma = \sigma_o + kR^{0.25} \tag{4}$$

where σ_o and k were functions of the sense of the applied stress. However, since $\lambda^2 R$ = const, both the tensile and compressive yield stresses were linearly dependent upon the inverse square root of the interlamellar spacing. Nevertheless, it seems advisable, in accordance with Chadwick's analyses,[94] to reserve a Hall-Petch plot of strength vs. $\lambda^{-1/2}$ to those cases where only a single strengthening mechanism operates, and where a dislocation pile-up model is applicable to the physical situation.

Thermally induced residual stresses due to the difference in thermal expansion coefficients, $\Delta\alpha$, of the two phases also may cause deviations from Eq. 2. These stresses are proportional to the product of the difference between the test temperature and the stress relaxation temperature, ΔT, and $\Delta\alpha$, and may reach very high values at room temperature. (Residual stresses will be further discussed in the section on compressive properties.) Finally, a deviation from the rule of mixtures may occur if there is a large spread in the strength of reinforcing fibers due to structural or geometrical defects. Rosen[10] considered this problem for artificial composites when he found that, in a composite reinforced with fibers, a fiber will break at different stress levels due to a distribution of flaws along the fiber length. The strength of the composite is obtained from a distribution function. In order to apply this model the distribution function must be determined experimentally by tensile tests performed on isolated fibers, an extremely difficult task for eutectic composites.

2. Post-Solidification Heat Treatments

The room temperature tensile strengths of Nitac[11] and γ/γ'-δ[12] type alloys can be increased by precipitation of the γ' phase from solution. Such aging treatments can produce increased strength over a wide range of test temperatures, as for example in the γ/γ'-δ alloy (6%Cr), shown in Fig. 4.[12] In addition, precipitation hardening has been successfully applied to Cotac.[13] Improvements in stress-rupture properties of Cotac by precipitation of small TaC particles is discussed in a succeeding section.

The strength of eutectic composites remains rather high with increasing test temperature until the melting point is approached. Data are shown in Fig. 5 for a γ'/γ-δ (Ni,Al,Mo) alloy.[14] The yield stress actually increases between 25°C and 700°C, as is characteristic of alloys containing γ' as one of the coexisting phases. The anamolous increase in yield stress of γ' with temperature also is partially responsible for the good strength retention of aligned eutectics shown in Fig. 2.

3. Strain Rate Effects

Substantial increases in yield and ultimate strengths at high strain rates (10^3 sec^{-1}) have been reported for aligned Al-Al_3Ni[15] tested in compression at room temperature and Al-Al_3Ni[16] and γ/γ'-δ[16] tested in tension at several test temperatures. The strain rate sensitivity of both alloys is significantly greater than for aluminum and other unalloyed fcc metals. However, the deformation and fracture characteristics of both alloys seem to depend primarily upon the response of the matrix to high strain rates. No change in fracture mode was observed at high strain rates, but ductility of Al-Al_3Ni tended to increase with strain rate; no effect

of strain rate on ductility of γ/γ'-δ was noted.[16]

4. Off-Axis Properties

It is well known that off-axis properties of artificial composites are inferior to those of the longitudinal orientation. Reductions in transverse strength for several alloys at three temperatures are shown in Fig. 6, expressed as the ratio of transverse to longitudinal tensile strength.[2] However, the γ'/γ-Mo eutectic (alloy AG-15, Table 1) for which the ratio is about 0.5 at 25°C, exhibits a ratio of 0.82 at 800°C, and about 0.7 at 1100°C.[14] This improvement in off-axis properties can be significant for high temperature turbine applications. Transverse ductility also often is reduced, as shown in Fig. 7 for γ/γ'-δ (6%Cr).[17]

III. Compressive Strength

Strengthening by interphase boundaries occurs in compression as well as in tension, presumably by similar mechanisms. However, differences in tensile and compressive strengths have been noted in several eutectic systems. The reasons for this anamolous behavior may be summarized as follows:

1) residual tensile stresses in the matrix produced by non-uniform thermal contraction of the two phases from the melting point result in a higher compressive yield stress.

2) twinning may occur in one direction and be suppressed in the other.

3) kinking or micro-buckling of fibers may occur in compression.

The residual stress mechanism has been attributed particularly to carbide-reinforced alloys, in which there is a large mismatch between

thermal expansion coefficients (Table 3).[18] For the (Co-Cr)-$(Co,Cr)_7C_3$ eutectic the proportional limit in compression is twice the proportional limit in tension.[19] Thermally induced prestressing due to the difference in thermal expansion coefficient between the two phases appears to be responsible. The Co-Cr solid solution expansion coefficient is higher than that of the carbide fibers. Therefore, at room temperature and in the absence of any external stresses, the matrix is in a state of tension and the fibers in compression. Since the residual thermal stress in the matrix is tensile, it will favor premature plastic deformation during tension at room temperature, whereas in compression the yield stress will be higher. On this model, the difference between the elastic limits in tension and compression should decrease when the temperature increases and vanish when the test temperature reaches the stress relaxation temperature; this is observed experimentally.[19]

Anisotropy of twinning with respect to stress direction contributes to yield stress differences in tension and compression in Ni-Ni_3Nb,[20] Cd-Zn[8] and Mg-$Mg_{17}Al_{12}$.[21] In tension, the Ni-Ni_3Nb composite first deforms by extensive {112} twinning, followed by cracking of the twin boundaries. In compression, the Ni_3Nb lamellae do not undergo deformation by {112} twinning; instead only {011} twins are found. The latter twins show no tendency to nucleate cracks at twin boundaries. It may be concluded that the superior compressive strength was due to the absence of a compressive deformation mechanism leading to cracking at twin boundaries, as had been observed in tension. In the case of Cd-Zn, twinning occurs readily in tension, but in compression Zn lamellae are required to buckle as a result of non-basal slip which occurs only at high stress levels. Consequently, the compressive

yield stress is higher than the tensile yield stress.[82]

Yue et al.[22] showed that the yield stress in compression of the Al-$CuAl_2$ eutectic is considerably higher than in tension, and can be further increased by post-solidification heat treatment. The anisotropy of yield strength was attributed to buckling of the fibers in compression only, with both matrix and fiber properties defining the buckling mode. Possible effects of heat treatment on the anisotropy of yielding apparently have not been reported for nickel or cobalt-base alloys.

IV. Creep and Stress Rupture

Aligned eutectics are characterized by excellent creep and stress rupture properties, as may be noted in Fig. 8, which compares several eutectics to a conventional nickel-base superalloy.[23] Additional data comparing stress rupture properties of several nickel-base alloys: γ/γ'-δ (6%Cr), Nitac 13, γ'-Ni_3Ta and two $\gamma/'\gamma$-Mo alloys (AG-15 and AG-34), (composition shown in Table 1) are compiled in Fig. 9.[14,23] At the high temperature, low stress end of the curve the five alloys are nearly equivalent, while at high stresses Nitac 13 and γ/γ'-δ are superior. However, Woodford[24] has shown that extensive oxidation of Nitac 13 occurs in air, particularly in long time tests. This leads to a breakdown of the Larson-Miller parameter correlation at the low stress end of the curve, see Fig. 10. An alternative parameter:

$$F(\sigma) = T\left(\frac{2000}{\sigma} + \log t_R\right) \qquad (5)$$

where σ is stress, T is temperature, °K, and t_R is rupture time was shown to describe air and argon data extremely well.[24]

The relation between steady-state creep rate, $\dot{\varepsilon}$, and the experimental variables of stress, σ, and temperature, T, is usually expressed by an exponential relation:

$$\dot{\varepsilon} = A\sigma^{n} e^{-Q/RT} \tag{6}$$

Typical values of the creep exponent, n, are 3-5 for most metals and alloys. However, for eutectic alloys values of n range from about 7 to 21, see Table 4. More recent data indicate that n is stress dependent in the low temperature Ag_3Mg-AgMg[25] and Pb-Sn systems[26] and is temperature dependent for γ/γ'-Cr_3C_2.[83] Therefore, Eq. 6 may not be the most suitable formulation for creep rate of eutectics. Activation energies for creep of eutectics also tend to be higher than for conventional alloys, perhaps due to slowed diffusion in the ordered intermetallic compounds which often are reinforcing phases.

The high sensitivity of creep rate to stress in aligned eutectics may arise from a type of dispersion-strengthening effect. Ansell and Weertman[27] predicted an exponential dependence of steady-state creep on stress in fine-grained two-phase alloys as follows:

$$\dot{\varepsilon} = A \exp\left[-Q(\sigma)/RT\right] \exp\left[B\sigma/RT\right] \tag{7}$$

where A is a constant, B is $-(dQ/d\sigma)$, and Q, the energy required to free dislocations from a boundary, is stress-dependent and decreases with increasing stress. Their model assumes restricted dislocation mobility with a large number of available dislocation sources at high applied stresses in fine-grained alloys. In conventional systems containing a constant number of dislocation sources, the rate of dislocation generation

is controlled by the movement of previously generated dislocations away from the sources. However, in cases where the slip distance is severely restricted and dislocation generation occurs from a large number of dislocation sources (as in fine-grained alloys), the rate of dislocation generation is assumed to be controlling. Similarly, this mechanism may apply to eutectic composites to explain the high sensitivity of steady-state creep rate to stress.

Recent work has shown that decreasing interphase spacing or fiber radius results in greatly enhanced creep resistance for several alloys; examples are shown in Fig. 11a) for rupture life of γ/γ'-δ[28] and Fig. 11b) for minimum creep rate of γ/γ'-Cr_3C_2,[29] both at 980°C. The proportionality between log $\dot{\varepsilon}$ and $1/\lambda$ of Fig. 11b) [λ is fiber radius] was consistent with a model based upon partitioning of the applied stress between matrix, fibers and an interface zone with creep resistance intermediate between those of matrix and fibers. The beneficial aspects of increasing growth rate to refine λ continues so long as structure is well aligned. Cellular microstructures obtained at high growth rates lead to inferior stress-rupture properties. Off-axis creep properties also tend to be less attractive as shown, for example, in Fig. 12 for γ'/γ-Mo.[14]

Apart from increasing the solidification rate, post-solidification heat treatments may be utilized to reduce creep damage. For example, heat treatment to precipitate carbides between the TaC fibers results in major improvement in stress rupture resistance of Co,Cr,Ni-TaC alloys (compare aged Cotac 33 to Cotac 3, the same alloy but unaged), see Fig. 13.[30]

V. Fatigue

The fatigue resistance of aligned eutectics, both at ambient and at

elevated temperatures is generally reported to be outstanding. Among high temperature fibrous alloys which have been tested are Cotac,[4,11,31] Nitac,[4,11,32] Ni-W[33] and γ/γ'-Cr_3C_2,[34] while fatigue properties of the lamellar nickel-base alloys Ni-Cr,[35] γ-δ,[36] γ'-δ[37] and γ/γ'-δ[32,38] also have been reported. Most of the work has been carried out in the high cycle range on unnotched samples, either in tension-tension or reversed bending, but some data on low cycle fatigue, notably for Ni-Cr[39] and Nitac[40] also are available. A few general patterns of behavior have emerged from these studies:

a) Fatigue cracking is usually controlled by the properties of the matrix; those factors which increase the strength of the matrix improve the fatigue resistance.

b) Decreasing interphase spacing through more rapid solidification produces significant improvements in fatigue life, but not necessarily at all test temperatures or stress levels.

c) Fatigue cracking in the matrix of fibrous eutectics and throughout lamellar eutectics is usually crystallographic (stage I) in nature. However, striations characteristic of stage II fatigue cracking also have been noted in several alloys.

These features of fatigue in eutectics will now be discussed in more detail.

Table 5 summarizes fatigue data for several nickel and cobalt-base eutectic alloys, the compositions of which appear in Table 1. All tests were conducted in tension-tension. A comparison of endurance limits for the various alloys shows that several of the alloys have room temperature endurance limits which are considerably in excess of those for many

conventional superalloys; at temperatures to 800°C, the eutectics continue to exhibit superior properties, particularly when endurance limits are expressed as a fraction of tensile strength. (It should be noted that data for eutectics are generally obtained in tension-tension cycling, which contributes to their apparent superiority.) Ratios of fatigue limit to tensile strength of up to 0.60 are noted in Table 5 for Cotac alloys, and up to 0.84 for γ/γ'-δ (0%Cr).[32] However, γ/γ'-δ alloys with 6%Cr are not as resistant to fatigue, for reasons which will be discussed below. It has been shown also that carbide-reinforced aligned eutectics are superior in fatigue to alloys with dispersed carbides.[4]

The excellent fatigue resistance of aligned eutectics has been attributed to several factors:

a) Accommodation of plastic strain in strong, ductile matrix materials.

b) The presence of debondable interfaces that cause crack branching.

c) High load-carrying capacity of reinforcing phases.

Interface cracking seems to be more prevalent in γ/γ'-δ type alloys than in carbide-reinforced eutectics tested in fatigue, and, therefore, may be the most significant of the above factors in explaining the high fatigue resistance of the former.[32,48]

In high-stress, low-cycle fatigue, failure of these alloys is a consequence of rupture of the reinforcing phase, which fractures ahead of the advancing crack. Cracks initiate at broken fibers in Nitac[40] and Cotac[31] although previous work had suggested that cracks originate in the matrix.[4] At low cyclic stresses or strains, cracks initiate in most eutectics

in slip bands and slip band extrusions. Fibers are later cracked by the impingement of these slip bands along their length.

We shall now consider the influence of specific microstructural variables on fatigue behavior.

a) Fiber Length and Orientation Effects

Most fatigue data reported in the literature for aligned eutectics were obtained from tests in which the cyclic stress was applied parallel to the growth direction of the samples (i.e., parallel to the fibers or lamellae). Anisotropy of mechanical behavior is a characteristic of all composites, and substantial effects on tensile properties of eutectics have been demonstrated, as for example in Figs. 6 and 7. The evidence in fatigue is conflicting: little influence of orientation on stress-controlled fatigue life of directionally solidified Al-Al_3Ni has been found;[41,42] for Co,Cr,Ni-TaC (Cotac), on the other hand, there is a decrease in fatigue limit of about 33% as the orientation of fibers changes from parallel to perpendicular to the stress axis.[4] More recently, Austin et al.[43] have measured crack propagation rates in Cotac, and report that transverse loading leads to a higher crack propagation rate for applied stress intensities above 15 MN $m^{-3/2}$, while below this critical value there is no effect of fiber orientation. Therefore, crack initiation must occur more readily in transverse orientations in order to influence the endurance limit. The fatigue limit of the latter is comparable to that of a notched parallel orientation sample.

There is some question as to the importance of fiber ends in promoting fatigue failure. Preferential crack propagation in Al-Al_3Ni at the ends of discontinuous fibers was not observed,[44] but for Fe-Fe_2B the stress

concentration at fiber ends was considered to favor fiber rupture ahead of the advancing crack.[45] There also is some controversy in the literature as to the influence of intentional prestrain on fatigue resistance. Bibring[4] reported a reduction in the room temperature rotating bending endurance limit of some 30% with precracking for Cotac, while Koburger et al[31] found an effect only at intermediate stress levels, see Fig. 14. At 1000°C, however, there is a considerable drop in fatigue resistance plus an additional drop due to precracking,[31] also shown in Fig. 14.

b) Interphase Spacing

It has been shown that finer microstructures lead to improved mechanical behavior under monotonic loading (tension, compression, or creep), provided that the test temperature is below that at which interphase boundary sliding may occur.

Decreasing λ has now been shown to improve high cycle fatigue resistance at room temperature of several eutectic alloys, including $\gamma/\gamma'-\delta$ and Cotac.[32] Data for $\gamma/\gamma'-\delta$, Fig. 15, reveal improvements in life at relatively high stress levels, but with no apparent effect on fatigue limit. In Cotac, on the other hand, an increase in growth rate from 0.6 to 2.5 cm/hr leads to a significant increase in fatigue life at all stress levels, see Fig. 16.[32] Note also the superiority of the aligned alloys to a Co,Cr,Ni solid solution with composition near that of the eutectic matrix. Fatigue limit data for several Cotac alloys and the solid solution Co,Cr,Ni alloy are tabulated in Table 6.[46] Note that Cr additions seem to have little effect on endurance limits, in marked contrast to a sharp drop in fatigue resistance of $\gamma/\gamma'-\delta$ with 6%Cr,

Fig. 15.[32] Bibring has reported, however, that significant changes in fatigue resistance of Cotac type alloys of varying Ni + Cr content are observed.[11,47] Consequently, fatigue resistance can be altered by compositional as well as microstructural factors. The decrease in fatigue resistance of γ/γ'-δ in the presence of Cr appears to be a consequence of the more imperfect microstructure, see Fig. 1b), as well as due to increased notch sensitivity relative to the 0%Cr alloy. Measured critical G/R values vary from 5°C hr cm^{-2} for chromium-free material to 150°C hr cm^{-2} at 6%Cr,[84] thereby accounting for the imperfect microstructure of the latter alloy.

c) Test Temperature

The influence of test temperature on fatigue life has been studied for Nitac (no Al)[40] and Ni-Cr[39] in strain-controlled cycling (low-cycle fatigue), as well as in γ/γ'-Cr_3C_2,[34] Nitac[4] and Cotac[4,31] in high-cycle fatigue. For γ/γ'-Cr_3C_2 at 800°C, the fatigue resistance at some stress levels is actually higher than at room temperature.[34] Unbroken fibers in γ/γ'-Cr_3C_2 bridge cracks in the matrix and prolong fatigue life at low stresses. Increasing temperature to 1000°C resulted in a sharp decrease in fatigue resistance of Cotac in air, Fig. 14, as discussed above.

d) Post-Solidification Heat Treatments

Improvements in room temperature fatigue resistance of Cotac,[4] Nitac[32] and Ni-W[33] are achievable through post-solidification heat treatments. Table 6 and Fig. 16 show that precipitation of carbides in Cotac increases the 10^7 cycle fatigue limit by 25%.[46] Data for Nitac in three conditions: as-directionally solidified, in the solution treated condition, and aged to precipitate γ', reveals that the aging treatment may

have a beneficial effect on fatigue lives at intermediate stress levels.[32] For Ni-W, the fatigue life at all values of σ_{max}/σ_y is increased substantially by an aging treatment, as shown in Fig. 17.[33] Failure in as-quenched Ni-W begins at a single surface origin, while multiple origins are found in aged samples. Ample evidence of effects of precipitates on the relative ease of crack initiation and propagation were noted and related to changes in slip character.

e) Crack Propagation

Fatigue crack propagation data have been reported only for the Ni-Ni_3Nb (γ-δ),[36] Cotac[32,43] and γ/γ'-δ eutectics.[38] A power relation,

$$da/dN = C\Delta K^m \qquad (7)$$

was established between crack growth rate and stress intensity over a range of crack growth rates from $5x10^{-9}$ m/cycle to $5x10^{-5}$ m/cycle for each of the alloys, as shown in Fig. 18. The data for the eutectic alloys, including the respective slopes, m, are analogous to those for steel alloys with comparable elastic moduli. Crack growth rates in γ/γ'-δ increase slightly with Cr additions, and also with increasing test temperature above 760°C, see Fig. 19.[38] However, no effect of λ on crack growth rate was reported in the range 427-927°C. The stress intensity range for the γ-δ system is a much more important factor than the mean stress intensity level.[36] However, a significant increase in da/dN with increasing stress ratio, R, has been found for Cotac.[43] Fatigue properties of γ-δ alloys with non-aligned structures are inferior to those of alloys in the aligned condition, as has previously been observed in Cotac. The crack propagation rate is further diminished in aligned specimens by producing δ-Ni_3Nb phase precipitates of Widmanstatten morphology within the Ni-rich

γ matrix as a result of an age-hardening treatment.[36]

Stage I (crystallographic) crack propagation has been noted in Cotac[4,31] and Nitac,[4,32] see Fig. 20, as well as in γ-δ,[36] and γ/γ'-δ.[32,48] For γ/γ'-δ there seems to be less tendency for stage I cracking when Cr is absent.[32,48] At high growth rates, Ni-W,[33] γ-δ[36] and Nitac,[32] Fig. 21, exhibit fatigue striations. The striation spacings in γ-δ are in good agreement with macroscopic growth rates.

For Ni-Cr, a wavy crack path through the nickel-rich phase is observed at temperatures below 500°C;[39] at higher temperatures, cracking is predominantly along the lamellar interface. Interfacial cracking also is prominent in γ/γ'-δ.[48] These results clearly demonstrate that crack paths in aligned eutectics can be sensitively affected by microstructure.

f) Cyclic Hardening and Softening

Measurements of cyclic-hardening phenomena in eutectics has been confined to high-strain experiments in lamellar Ni-Cr[35,39] and in fibrous Ni,Cr-TaC alloys.[40] Investigations on both alloys were conducted in tension-compression at room temperature and at elevated temperatures. The stress-strain hysteresis loop for Ni,Cr-TaC is very different from that of conventional alloys in that the shape of the loops depends on whether or not fibers crack in the early stages of cyclic strain. Consequently, the shape of the loops may be used as a measure of fiber integrity.

The Ni-Cr alloy, in both the as-cast and aligned conditions, exhibits cyclic-strain hardening at all temperatures in the range from 300°C to 760°C.[39] However, there is a well-defined saturation stress following initial hardening only for temperatures above 500°C. There also is an apparent softening after about 90% of total life at 500°C and after about

75% of total life at 625°C. This may be related to crack propagation rather than substructural instability. As-cast material, on the other hand, reveals no softening.

g) Low-Cycle Fatigue

A comprehensive investigation[40] of low-cycle fatigue in a simple Nitac alloy (Ni,10Cr-TaC) has shown that the Coffin-Manson relation between plastic strain range $\Delta\varepsilon_p$ and life is observed:

$$N_f \Delta\varepsilon_p^{1/2} = \text{constant}.$$

The low-cycle fatigue resistance of this alloy was shown to be superior to that of Rene' 80, a cast nickel-base superalloy, at 870°C. Other low-cycle fatigue data have been reported for Ni-Cr.[39]

VI. Thermal Fatigue

Potential application of aligned eutectics in aircraft gas turbines has led to considerable interest in the properties of these alloys under conditions of repeated thermal cycling.[4,18,49,50] Unfortunately, there has been no general agreement as to the type of laboratory test which most nearly simulates thermal fatigue under aircraft operating conditions. Damage accumulation may be a result of microstructural changes induced by internal strains due to thermal expansion mismatches, see Table 3, or by γ' precipitation in nickel alloys. Alloy compositional changes can have a pronounced influence on microstructural instabilities, as for example when nickel is added to cobalt-base alloys to suppress the fcc-hcp phase transformation.

One method of testing involves repeated rapid thermal cycles with

little or no hold times, while another group of experiments is conducted at lower rates and with hold times. Gray and Sanders[51] have reported that γ/γ'-δ (6%Cr), while subject to γ' coarsening and Widmanstatten δ precipitation in the γ phase, exhibits little change in mechanical properties after exposure in a burner rig for 3000 "rapid" cycles between 425°C and 1100°C. However, the already poor oxidation resistance of this alloy was further degraded by the burner rig exposure. Leverant[52] has noted little effect of thermal cycling with appreciable hold times between 120°C and 1037°C on creep rupture properties of this alloy. Overlay coated samples of γ/γ'-δ (6%Cr) exhibited life during cycling between 427°C and 1038°C that was similar to that of B-1900, a conventionally cast Ni-base superalloy.[53] Crack growth rates for γ/γ'-δ under these conditions were slightly lower than for B-1900, but were higher than for DS MarM-200, another conventional superalloy. The carbide reinforced eutectics exhibit wide ranges of behavior as a result of thermal cycling. Ni-NbC, Ni,Cr-NbC, Co,Cr-NbC and Co,Cr,Ni-TaC were reported by Breinan et al[49] to be severely damaged by thermal cycling between 400°C and 1121°C in two minutes by self-resistance heating; however, Bibring[4] reported, to the contrary, that Nitac and Cotac alloys suffer little damage as a result of cycling between 23°C and 1000°C, both with and without simultaneous loading. Heavily alloyed Nitac showed no microstructural changes after 3000 cycles between 400°C and 1120°C.[54] Woodford[55,56] has shown that cobalt alloys are inherently less stable to thermal cycling than nickel-base alloys, due to the occurrence of the hcp-fcc phase transformation and the extremely planar slip characteristics of the former. Moreover, property degradation occurred even in the absence of losses in fiber integrity. Cobalt alloys may be

improved, however, by adding nickel to suppress the phase transformation and by utilizing fine precipitates to disperse slip and inhibit recovery.

Nitac 13 is at least as stable to temperature cycling as two conventional nickel-base superalloys: Rene' 80 A and Rene' 80 B, and much superior to Co50B3W for cycles in excess of 600, see Fig. 22.[55] However, after only 200 cycles, the Co-base alloy actually doubled in strength, relative to the uncycled condition; the strength then fell precipitously with further cycling. The balance between initial hardening due to cycling and subsequently softening (recovery) will depend upon T_{max}, the temperature range ΔT, and the cycle shape and period, as well as the magnitude of the applied stress.[56]

An alternative means of assessing thermal cycling resistance is to measure the creep rate as cycling progresses. No effect of thermal cycling between 250°C and 982°C has been observed on creep curves of γ/γ'-δ (R = 3 cm/hr), but there is some evidence of degradation on cycling from 1038°C.[53] Limited data of Bibring[13] on the same alloy also indicated some acceleration of creep under thermal cycling, but the magnitude and reproducibility of the effect were not established. Woodford[56] has provided an incremental analysis of creep strain accumulation under thermal cycling which predicts that the creep strain should be sensitive to cycle period. Creep strain could be predicted within about 25%.

Some promising developments in the design of thermal fatigue-resistant eutectics have recently been reported. A new cobalt-base alloy: Co,15Cr,20Ni-10.5Hf,0.7C subjected to thermal cycling between 425°C and 1100°C, utilizing a 2.5 minute cycle, revealed no microstructural degradation of fibers after 2500 cycles.[57] Similar stability against

thermal cycling has been reported for a Ni-10C-5Al-8.3Hf-1.1Zr-0.7C alloy.[58] Two nickel-base alloys reinforced with NbC fibers: "Cotac" 74 and "Cotac" 471, in which the nickel matrices are precipitation hardened by γ' and solid solution strengthened by tungsten have demonstrated superior thermal cycling resistance.[59] Cycles imposed between 250°C and either 1070°C or 1100°C, with an applied stress of 120 MN/m^2 and a hold time at T_{max} of 28 minutes produced stress rupture lives within 20% of those obtained in isothermal tests. Additional rapid cycle tests performed on these alloys resulted in equally good properties: for Cotac 74 the loss in 1070°C tensile strength after 5000 prior cycles was about 18%, and for Cotac 741 about 15%. Metallographic examination of both alloys after 5000 cycles at 1070°C revealed little degradation of fibers, consistent with the tensile results. The apparent superiority of HfC and NbC as fiber reinforcements, relative to the more widely studied TaC-strengthened alloys, may arise from lower solubility changes with temperature and more favorable thermal expansion mismatches in addition to the higher strengths of the matrices of the new alloys.

The various experimental results reported above, together with the analytical approaches of Garmong[60-62] and Woodford[56] illustrate the complexity of the thermal cycling problem. It is certain that test variables as well as material characteristics must be carefully evaluated when comparing test results from different laboratories. Thermal expansion differences, solubility changes and matrix strength appear to be the most significant material properties, while applied stress (or strain), T_{max}, ΔT, and cycle time are the most important test variables.

Another illustration of thermal stability problems that may be

encountered with certain alloys is provided by work on Nb-Nb_2C.[63] While isothermal stability was good on exposure to temperatures between 0.5 - 0.67 T_m, deformation of the alloy prior to annealing caused catastrophic spheroidization of the carbide.

VII. Impact Properties

Resistance to impact damage is important for structural design, and there are several alloys for which data are available. Jackson et al[64] have recently compared the room temperature impact energies of several nickel and cobalt-base aligned eutectics with that of Rene' 80. The results for Charpy V-notch specimens and sub-size specimens are summarized in Table 7.

The mini-specimens, which were of recommended ASTM modified designs, 5 mm x 5 mm cross section, with a 1 mm deep notch (ligament area = 1/4 of that of a standard specimen), revealed that γ'/γ-Mo (alloy AG-15, Table 1), was the toughest of all eutectic alloys studied. Based on comparisons with data for standard specimen sizes, all the eutectic alloys shown appear to be superior to the nickel-base superalloy Rene' 80. The impact energies of all eutectic alloys shown in Table 7 also are superior to those for δ-reinforced alloys such as γ'-δ and γ/γ'-δ,[65] see Fig. 23. Room temperature values for these alloys are near 2-4 joules, which is comparable to the impact resistance of MarM-200, a strong nickel-base superalloy. The γ/γ'-δ alloy exhibits a linear increase in impact energy absorbed to 1000°C, while the γ'-δ alloy reaches a peak at 1000°C and then declines. Bibring[4] has reported that unnotched Cotac has excellent impact resistance at temperatures ranging from 20° to 1000°C. An

important crack arrest mechanism in mechanically combined metal-matrix composites is the ability of a propagating crack to turn parallel to the interphase boundaries, thereby blunting transverse cracks and creating new surfaces among aligned eutectics. This behavior is particularly noteworthy in the case of γ'/γ-Mo alloys,[64] but is less important in other eutectics which possess a stronger interfacial bond. In those cases energy absorbed by the matrix ahead of the advancing crack probably plays a major role.

Another alloy for which considerable impact data have been reported is fibrous Co,Cr-$(Cr,Co)_7C_3$.[66,67] The maximum toughness for Co,Cr-$(Cr,Co)_7C_3$ is obtained in the orientation for which propagating cracks can cause longitudinal splitting of the carbide fibers; this orientation has the base of the notch at 90° to the fibers. In this orientation the toughness is about three times that of cast MarM-302. The minimum energy for fracture is in a transverse orientation. Another interesting feature of the impact strength of this alloy is a minimum in resistance between 200°C and 900°C.[67] Nicoll and Sahm[68] have recently reported that the impact strength of Co,Cr-$Cr_{7-x}Co_xC_3$ composites can be substantially improved at all temperatures below 1000°C by alloying with nickel. This result is apparently due largely to the ductilizing effects of nickel on Co or Co,Cr alloys, perhaps due to the increased stacking fault energy of the matrix.

VIII. Environment-Sensitive Mechanical Behavior

Potential applications of eutectic alloys in gas turbine applications has led to considerable interest in static and cyclic oxidation behavior of these materials. Much less interest has been directed to the influence of

environments on mechanical behavior at or near ambient temperatures. However, hydrogen has recently been shown to be an embrittling agent for certain eutectic alloys. Ni-45.5%W and γ/γ'-δ alloys are severely embrittled when tested in hydrogen gas,[69] while γ/γ'-δ (0%Cr) also suffers severe reversible embrittlement after cathodic charging.[70] For Ni-W the interphase boundaries are severely embrittled; boundaries are embrittled also in cathodic charging of γ/γ'-δ, but the major contributing factor to reduced ductility is eased propagation of cracks from the δ phase into the γ matrix along slip or twin bands.

IX. Applications

Several nickel-base eutectic composites offer a significant temperature advantage over conventional nickel and cobalt-base superalloys in terms of tensile, impact strength and creep rupture and fatigue resistance. Consequently, this class of alloys has been the object of intense development efforts at several aircraft engine laboratories, with the objective of producing improved stator or turbine blades, thereby permitting increased turbine inlet temperatures. There is little room for improvement of current superalloys in terms of alloy development. In fact, much of the increase in turbine operating temperatures achieved in recent years has been through development of turbine blade designs with increasingly complex internal and external air cooling, resulting in lower metal temperatures and thermal gradients.[87] The major candidate material systems for continued increases in turbine inlet temperatures include refractory metals, ceramics, mechanically incorporated (synthesized) composites and aligned eutectics. Oxidation problems with refractory metals and brittleness of ceramics are

obstacles which many years of effort have failed to overcome. The synthesized composites, of which nickel with tungsten wires is an example, generally suffer from chemical reaction between fiber and matrix although quite high strengths have been achieved. However, the aligned eutectics are at or near thermodynamic equilibrium at elevated temperatures, and therefore exhibit superior microstructural stability. Under thermal cycling conditions this stability is degraded, but Woodford's results[56] show clearly that nickel-base eutectics probably do not suffer any more degradation than conventional superalloys. Acceptable ductility (at least 6% over the entire temperature range) as well as densities below 9 Mg/m^3 have been achieved in several eutectic alloys,[88] and continued improvements are being announced in thermal cycling resistance.[57-59]

Some major drawbacks to application of eutectics in gas turbines include the critical importance of development of a carefully controlled microstructure, and the markedly anisotropic properties displayed by most alloys. However, there is reason for optimism even in these areas: improvement of properties through control of microstructure is a distinct advantage relative to synthetic composites, and efforts along these lines are at an early stage of development. Also, there are marked differences in the transverse properties of various alloys relative to their longitudinal properties, see Figs. 6 and 7 and ref. 14, suggesting that further alloy development may succeed in eliminating a substantial fraction of the problems arising from inadequate transverse strength and/or ductility. Another problem which is receiving considerable attention, although not addressed in this paper is surface protection. In all likelihood eutectic

composites would have to be coated in order to obtain adequate oxidation resistance. Studies are underway to solve this problem.

Perhaps the most vexing problem related to eutectic turbine blade development is concerned with achieving superior properties at an acceptable cost. The directional solidification process, even for solid blades, is expensive. If cooled blades are necessary the process becomes much more expensive, and the ability to maintain an aligned microstructure in routine casting of hollow blades is uncertain. However, Curran et al.[89] have successfully grown γ/γ'-δ (6%Cr) in cored airfoil form, using liquid metal cooling. The microstructure was lamellar in the airfoil section but cellular in the rod due to the large mass in the latter region.

Based on laboratory tests, the aligned eutectics show considerable promise as turbine or stator blade materials. For example, γ/γ'-δ offers a 55-80°C advantage in creep behavior over the advanced superalloy MarM-200+Hf.[89] Engine tests soon to be conducted at General Electric Co. on a nickel-base composite should give a more reliable estimate of the potential for eutectics in aircraft gas turbines.[91]

X. Summary

This review has been concerned almost entirely with the mechanical behavior of nickel and cobalt-base eutectic composites. For descriptions of the mechanical behavior of other eutectic alloys the reader is referred to a number of recent review papers.[2-4,92,93]

The mechanical behavior of nickel and cobalt-base aligned eutectics is characterized by high static and cyclic strengths, both at 25°C and at temperatures to 1100°C. Room temperature impact properties of carbide and

Mo fiber-reinforced several alloys are superior to those of conventional cast superalloys. Nearly all aligned eutectics are stable against isothermal coarsening to homologous temperatures up to 0.9 T_m. However, under thermal cycling conditions some carbide-reinforced eutectics, particularly cobalt-base alloys, undergo significant breakdown of their aligned microstructure, with consequent losses in tensile and creep-rupture strength. While much effort has been devoted to optimization of alloy properties through compositional control (alloy development), opportunities for improvements through microstructural control have received less attention. Reducing interphase spacing through increases in alloy solidification rate leads to improved tensile, creep and fatigue properties. The spacing effect may be most significant in fatigue at temperatures >0.5 T_m, where creep-fatigue interactions are likely. Post-solidification heat treatments to produce carbide or γ' precipitates have been shown to offer significant opportunities for improvements in tensile and creep strength, but of course this can only apply to a relatively small number of alloy systems. Fatigue properties also are improved by such treatments, but not under all test conditions. Further significant improvements in mechanical properties, particularly at elevated temperatures, are likely to be achieved when the significance of microstructural features is more widely recognized.

References

1. W. A. Tiller, in "Liquid Metals and Solidification," ASM, Cleveland, 1958, p. 276.
2. R. L. Ashbrook, in Directionally Solidified In-Situ Composites, AGARD-CP-156, North Atlantic Treaty Organization, 1974, p. 93.
3. M. R. Jackson, in Proc. Sec. Conf. on In-Situ Composites, Xerox, Lexington, Mass., 1976, p. 67.
4. H. Bibring, Proc. Conf. on In-Situ Composites, NMAB 308-II, National Research Council, Washington, D. C., 1973, p. 1.
5. M. Henry, in Proc. Conf. on In-Situ Composites, NMAB 308-II, National Research Council, Washington, D. C., 1973, p. 173.
6. F. D. Lemkey, "Eutectic Superalloys Strengthened by δ,Ni_3Cb Lamellae and γ',Ni_3Al Precipitates," United Aircraft Res. Labs., NASA CR-2278, Nov. 1973.
7. H. E. Cline and D. F. Stein, Trans. TMS-AIME, V. 245, 1969, p. 841.
8. B. J. Shaw, Acta Met., V. 15, 1967, p. 1169.
9. E. R. Thompson, F. D. George and E. M. Breinan, Proc. Conf. on In-Situ Composites, NMAB 308-II, National Research Council, Washington, D. C., 1973, p. 71.
10. B. W. Rosen, in Fiber Composite Materials, American Society for Metals, Metals Park, Ohio, 1965, p. 37.
11. H. Bibring, G. Seibel and M. Rabinovitch, Mem. Sci. Rev. Met., V. 69, 1972, p. 341.
12. S. N. Tewari and R. L. Dreshfield, ASME Preprint 76-GT-103, 1976.
13. H. Bibring, in Directionally Solidified Eutectic Composites, AGARD-CP-156, North Atlantic Treaty Organization, 1974, p. 141.

14. M. R. Jackson, J. L. Walter and M. F. Henry, Quarterly Report No. 3, Contract NAS3-19711, General Electric Co., Schenectady, N. Y., Dec. 1, 1975 - Feb. 29, 1976.

15. R. L. Sierakowski and F. D. Lemkey, in Proc. Conf. on In-Situ Composites, NMAB 308-II, 1973, p. 285.

16. R. Matera, C. Albertini and N. S. Stoloff, unpublished research.

17. K. D. Sheffler, R. H. Barkalow, A. Yuen and G. R. Leverant, Met. Trans., V. 8A, 1977, p. 83.

18. M. Gell, in Directionally Solidified In-Situ Composites, AGARD-CP-156, North Atlantic Treaty Organization, 1974, p. 117.

19. D. A. Koss and S. M. Copley, Met. Trans., V. 2, 1971, p. 1557.

20. W. R. Hoover and R. W. Hertzberg, Met. Trans., V. 2, 1971, p. 1289.

21. P. Hargraves and N. S. Stoloff, Rensselaer Polytechnic Institute, unpublished.

22. A. S. Yue, F. W. Crossman, A. E. Vidoz and M. I. Jackson, Trans. TMS-AIME, V. 242, 1968, p. 2441.

23. F. Mollard, B. Lux and J. C. Hubert, Z. Metallk., V. 65, 1974, p. 461.

24. D. A. Woodford, Met. Trans., V. 8A, 1977, p. 639.

25. Y. G. Kim and N. S. Stoloff, Met. Trans., V. 5, 1974, p. 809.

26. M. Suery, A. Eberhardt and B. Baudelet, et al, Proc. Sec. Conf. on In-Situ Composites, Xerox, Lexington, Mass., 1976, p. 481.

27. G. S. Ansell and J. Weertman, Trans. TMS-AIME, V. 221, 1959, p. 838.

28. M. Gell and R. H. Barkalow, in "The Microstructure and Design of Alloys", Proc. Third Int. Conf. on Strength of Metals and Alloys, Cambridge, V. 1, 1973, p. 261.

29. E. Bullock, M. McLean and D. E. Miles, Acta Met., V. 25, 1977, p. 333.

30. J. P. Trottier, T. Khan, J. F. Stohr, M. Rabinovitch and H. Bibring, Cobalt, 1974, p. 3.

31. C. Koburger, N. S. Stoloff and D. J. Duquette, Proc. Sec. Conf. on In-Situ Composites, Xerox, Lexington, Mass., 1976, p. 587.

32. N. S. Stoloff, W. A. Johnson, J. E. Grossman and C. Koburger, "High Cycle Fatigue of Nickel and Cobalt-Base Aligned Eutectics," Technical Report No. 2 to Office of Naval Research, Contract N00014-75-C-0503 NR 031-745, Aug. 1, 1976.

33. G. Garmong and J. C. Williams, Met. Trans. A, V. 6A, 1975, p. 1711.

34. G. J. May, Met. Trans., V. 6A, 1975, p. 1115.

35. R. Kossowsky, K. Sadananda and M. Doner, in Electron Microscopy and Structure of Materials, University of California Press, Berkeley, 1972, p. 764.

36. W. J. Mills and R. W. Hertzberg, in Fatigue of Composite Materials, STP 569, ASTM, Philadelphia, Pa.

37. E. R. Thompson, F. D. George and E. H. Kraft, Report No. J91086-4, United Aircraft Res. Labs., July 1970.

38. A. Yuen and G. R. Leverant, Met. Trans., V. 7A, 1976, p. 1443.

39. M. Doner, J. D. DiPrimio, and E. I. Salkovitz, Met. Trans., V. 5, 1974, p. 433.

40. M. F. Henry and N. S. Stoloff, in Fatigue of Composite Materials, STP 569, Philadelphia, Pa., 1975, p. 189.

41. G. E. Maurer, D. J. Duquette and N. S. Stoloff, Met. Trans., V. 7A, 1976, p. 703.

42. W. G. Ovens and A. J. McEvily, Proc. Conf. on In-Situ Composites, NMAB II, National Research Council, Washington, D. C., 1973, p. 273.

43. C. J. Austin, D. J. Duquette and N. S. Stoloff, accepted by Met. Trans., 1977.

44. W. R. Hoover and R. W. Hertzberg, Trans. ASM, V. 61, 1968, p. 769.

45. A. R. T. de Silva and C. A. Chadwick, Met. Sci. J., V. 4, 1970, p. 63.

46. C. J. Koburger, D. J. Duquette and N. S. Stoloff, Acta Met., 1977, to be published.

47. H. Bibring, J. P. Trottier, M. Rabinovitch and G. Seibel, Mem. Sci. Rev. Met., V. 68, 1971, p. 23.

48. J. E. Grossman and N. S. Stoloff, submitted to Met. Trans., 1977.

49. E. M. Breinan, E. R. Thompson and F. D. Lemkey, Proc. Conf. on In-Situ Composites, NMAB 308-II, 1973, p. 201.

50. G. Garmong and C. Rhodes, Proc. Conf. on In-Situ Composites, NMAB 308-I, 1973, p. 251.

51. H. R. Gray and W. A. Sanders, Proc. Sec. Conf. on In-Situ Composites, Xerox, Lexington, Mass., 1976, p. 201.

52. G. R. Leverant, discussion to ref. 51.

53. R. H. Barkalow, J. J. Jackson, M. Gell and G. R. Leverant, Proc. Sec. Conf. on In-Situ Composites, Xerox, Lexington, Mass., 1976, p. 549.

54. F. D. Lemkey, Fifth Annual Spring Meeting of AIME, Philadelphia, Pa., May 1973.

55. D. Woodford, Proc. Sec. Conf. on In-Situ Composites, Xerox, Lexington, Mass., 1976, p. 211.

56. D. A. Woodford, Mat. Sci. and Eng., V. 24, 1976, p. 257.

57. Y. G. Kim, Proc. Sec. Conf. on In-Situ Composites, Xerox, Lexington, Mass., 1976, p. 223.

58. Y. G. Kim, submitted to J. Materials Sci., 1977.

59. M. Rabinovitch, Ispra Course on Advances in Composite Materials, 25-29 Oct., 1976, Ispra (Varese) Italy.

60. G. Garmong, Met. Trans., V. 5, 1974, p. 2183.

61. G. Garmong, Met. Trans., V. 6A, 1975, p. 1179.

62. G. Garmong, in Proc. Sec. Conf. on In-Situ Composites, Xerox, Lexington, Mass., 1976, p. 137.

63. S. A. David, K. Y. Lin and H. D. Brody, Proc. Sec. Conf. on In-Situ Composites, NMAB-II, 1973, p. 223.

64. M. R. Jackson, J. L. Walter and M. F. Henry, Evaulation of DS Eutectic Superalloys for Turbine Blade Applications, Quarterly Report No. 4, Contract NAS3-19711, March 1, 1976 - May 31, 1976.

65. E. R. Thompson and F. D. George, Eutectic Superalloys, Paper No. 690689, New York, Soceity of Automotive Eng., 1969 (see also ref. 2).

66. E. R. Thompson, J. Composite Mat., V. 5, 1971, p. 235.

67. P. R. Sahm and T. Varga, Proc. Conf. on In-Situ Composites, NMAB-II, Washington, D. C., 1973, p. 239.

68. A. R. Nicoll and P. R. Sahm, Proc. Int. Conf. on Composite Materials, V. 2, Geneva, Switzerland and Boston, Mass., AIME, New York, 1976, p. 904.

69. G. Garmong, Met. Trans., V. 8A, 1977, p. 535.

70. N. S. Stoloff, L. Klein, J. E. Grossman and H. L. Marcus, in Scripta Met., V. 10, 1976, p. 889.

71. J. Tartaglia, Rensselaer Polytechnic Institute, unpublished.

72. P. Annarumma and M. Turpin, Met. Trans., V. 3, 1972, p. 137.

73. E. R. Thompson, D. A. Koss and J. C. Chessnut, Met. Trans., V. 1, 1970, p. 2807.

74. J. C. Hubert, F. R. Mollard and B. Lux, Proc. Conf. on In-Situ Composites, NMAB 308-II, National Research Council, 1973, p. 323.

75. A. Bassi, R. Matera, G. Piatti and D. Wenger, Mem. Sci. Rev. Met., V. 75, 1975, p. 171.

76. R. Kossowsky, Met. Trans., V. 1, 1970, p. 1909.

77. C. Koburger, D. J. Duquette and N. S. Stoloff, Acta Met., 1977, to be published.

78. N. S. Stoloff and D. J. Duquette, in Fractography-Microscopic Cracking Processes, STP 600, ASTM, Philadelphia, Pa., 1976, p. 154.

79. E. R. Thompson and F. D. George, Eutectic Superalloys, Paper No. 690689, Soc. of Automotive Eng., New York, 1969.

80. R. P. Gangloff and R. W. Hertzberg, Proc. Conf. on In-Situ Composites, NMAB 308-II, National Research Council, Washington, D. C., 1973, p. 83.

81. K. D. Sheffler, R. W. Hertzberg and R. W. Kraft, Trans. ASM, V. 62, 1969, p. 105.

82. M. Sahoo, R. A. Porter and R. W. Smith, J. Mat. Sci., V. 11, 1976, p. 1680.

83. D. E. Miles, E. Bullock and M. McLean, Proc. Sec. Conf. on In-Situ Composites, Xerox, Lexington, Mass., 1976, p. 539.

84. K. D. Sheffler, R. H. Barkalow, A. Yuen and G. R. Leverant, Proc. Conf. on In-Situ Composites II, p. 353, Xerox Publ. Co., Lexington, Mass., 1976.

85. K. Sadananda, J. C. DiPrimio and E. J. Salkovitz, Tech. Report, ARPA Contract No. DAHC-15-67-C-0176, 1969.

86. E. R. Thompson, F. D. George and E. H. Kraft, Final Report, Contract No. N00019-70-C-0052, July 1970.

87. L. P. Jahnke and C. A. Bruch , in AGARD-CP-156, North Atlantic Treaty Organization, 1974, p. 3.

88. M. G. Cockroft and P. H. Cowley, in AGARD-CP-156, North Atlantic Treaty Organization, 1974, p. 157.

89. P. M. Curran, L. F. Schulmeister, J. E. Erickson and A. F. Giamei, in Proc. Sec. Conf. on In-Situ Composites, Lexington, Mass., 1976, p. 285.

90. C. Bathias and R. M. Pelloux, Met. Trans., V. 4, 1973, p. 1265.

91. M. F. Henry, Geisler Memorial Lecture, Colonie, New York, 1977.

92. W. Kurz and P. R. Sahm "Gericktet erstarrte eutektische Werkstoffe," Springer-Verlag, Berlin, 1975.

93. A. Lawley, in Proc. Sec. Conf. on In-Situ Composites, Lexington, Mass., 1976, p. 451.

94. G. A. Chadwick, Met. Sci. J., V. 9, 1975, p. 300.

Table 1

High Temperature Eutectic Alloy Compositions

Alloy	Morphology	V_f	w% Solute								
			Ni	Co	Cr	Al	Nb	Mo	Ta	C	Other
Nitac	F	0.05	69	--	10	5	--	--	14.9	1.1	--
Nitac 13	F	--	63	3.3	4.4	5.4	--	--	8.1	0.54	3.1W,6.2Re,5.6V
Cotac 74	F	--	bal	20	10	4	4.9	--	--	0.55	10W
Cotac 741	F	--	bal	10	10	5	4.7	--	--	0.5	10W
Cotac	F	0.10	10	65	10	--	--	--	14	1	--
Cotac 3 or 33*	F	0.10	10	56	20	--	--	--	13	1	--
Cotac 50B3W	F	0.10	9.5	59	15.7	--	--	--	12	0.77	3W
γ/γ'-δ (6%Cr)	L	0.37	71.5	--	6	2.5	20	--	--	--	--
γ/γ'-δ (0%Cr)	L	0.3	76.5	--	--	2.5	21	--	--	--	--
γ'/γ-Mo (AG-15)	F	0.26	65.5	--	--	8.1	--	26.4	--	--	--
γ'/γ-Mo (AG-34)	F	0.26	62.5	--	--	6.3	--	31.2	--	--	--
γ-δ	L	0.26	66.7	--	--	--	23.3	--	--	--	--
Ni_3Ta-Ni_3Al	L	0.35	64.1	--	--	4.9	--	--	31	--	--
Co,Cr-$(Co,Cr)_7C_3$	F	0.30	--	56.6	41	--	--	--	--	2.4	--
γ/γ'-Ni_3Ta	L	--	67.6	--	--	3.7	--	--	28.7	--	--
Ni-Ni_3Ta	L	--	63	--	--	--	--	--	37	--	--
γ'-δ	L	0.44	bal	--	--	4.4	23.4	--	--	--	--
Co,Cr-$(Cr-Co)_7C_3$	F	0.3	--	bal	41	--	--	--	--	2.4	--

* 1300°C, 2hr; 1000°C, 24hr, A.C.

Table 2

Longitudinal Tensile Properties of As-Grown Aligned Eutectics, 25°C

Alloy**	Type	T_m °C	ρ g/cc	R cm/hr	σ_y MN/m²	σ_y ksi	σ_{UTS} MN/m²	σ_{UTS} ksi	% Elong.	Ref.
Nitac	D-B	1348	∿8.8	0.6	814*	118*	1304	189	54	32
Nitac 13	D-B	--	--	0.6	--	--	1420	205	--	14
Cotac 74	D-B	1335	8.6	--	1260*	182.6*	1550	225	12.4	59
Cotac (Co,Cr,Ni-TaC)	D-B	1402	9.0	0.6	787*	114*	963	139.5	30	31
Cotac (Co,Cr,Ni-TaC)	D-B	1402	9.0	2.5	842*	122*	1042	151	33	32
γ/γ'-δ (0%Cr)	D-SB	1272-1274	--	3	814	118	1193	173	∿30	32
γ/γ'-δ (6%Cr)	D-SB	1244-1257	8.6	3	649	94	1187	172	3.0	32
γ'/γ-Mo (AG-15)	D-D	1306	8.2	1.9	621	90	1346	195	21.9	71
γ'/γ-Mo (AG-34)	D-D	--	--	0.76	580	84	1446	209.6	19.2	71
γ'-δ	D-SB	1280	8.5		1035	150	1242	180	<1	6
γ-δ	D-SB	1270	--	0.6-4.5	428	62	863	125	22	72
Co,Cr-$(Co,Cr)_7C_3$	D-B	1330	8.0		828	120	1380	200	<2	73
Ni_3Ta-Ni_3Al	B-D	∿1360	--	1.33	690	100	725	106	<1	74
γ/γ'-Ni_3Ta	D-B	∿1360	--	1.33	916	132.9	984	142.7	2.8	23
γ-Ni_3Ta	D-B	1360	11.1	0.5	962	139.4	962	139.4	--	75

* fiber fracture stress (upper yield stress)

** Matrix phase listed first.

Table 3

Approximate Thermal Expansion Mismatch Between Phases of Some D.S. Eutectics[18]

D. S. Eutectic	Average Thermal Expansion Mismatch (°C)
Ni-NbC	$10. \times 10^{-6}$
Ni,Cr-NbC	9.4×10^{-6}
Co,Cr-NbC	9.4×10^{-6}
Co,Cr,Ni-TaC	9.9×10^{-6}
Ni,Cr-TaC	9.9×10^{-6}
Ni,Cr,Al-TaC	8.1×10^{-6}
Ni_3Al-Ni_3Nb (γ'-δ)	1.6×10^{-6}
(Ni,Cr) (Ni_3Al)-Ni_3Nb, (γ/γ'-δ)	6.1×10^{-6}

Table 4

Creep Parameters for Aligned Eutectics

Alloy	Stress Exponent	Activation Energy (Kcal/mole)	Ref.
Co,Cr-$(Co,Cr)_7C_3$	7	135-150	73
Ni_3Al-Ni_3Nb	4-8	129-173	9
Ni-Cr	7	80	76
Ni-Ni_3Nb	21	--	80
Ni-Ni_3Ti	--	100	81
Co,Cr-TaC	--	130	4,47
γ/γ'-Cr_3C_2	4.8-8.8*	68-187*	83

* temperature dependent

Table 5

Comparison of Fatigue Limits of Aligned Eutectics, 25°C

	R cm/hr	Condition	σ_{UTS} MN/m^2	$\Delta\sigma_{10^7}$ MN/m^2	$\frac{\sigma_{max_{10^7}}}{\sigma_{UTS}}$	Ref.
Nitac	0.6	as-D.S.	1304	518	0.42	32
"	0.6	solution treated	1249	483	0.41	32
"	0.6	aged	1228	--	--	32
Cotac	0.6	as-D.S.	963	518	0.57	31
"	2.5	as-D.S.	1042	690	0.7	46
γ/γ'-δ(0%Cr)	3	as-D.S.	1193	966	0.84	32
"	5.7	as-D.S.	--	966	--	32
γ/γ'-δ(6%Cr)	3	as-D.S.	1187	656	0.58	32
Ni-Cr	--	as-D.S.	~828	587	0.71	85
γ-δ	4.7	as-D.S.	745	414*	0.56*	20
γ'-δ	--	as-D.S.	1173	690	0.59	86
Ni-W	3.0	as-quenched	920	350	0.38	33

*Notched

Table 6

Fatigue Properties of Cotac, 25°C[31,46]

(Co,10Cr,10Ni-TaC)

	R	λ	σ_y (0.2%)	Fiber Fracture Stress	UTS	ε_F	10^7 Cycle Limit Δσ
	cm/hr	μm	ksi	ksi	ksi	%	ksi
Co,Cr,Ni-TaC	as-cast	--	57	--	142	5	55
Co,Cr,Ni-TaC	0.63	5	70	108	139	30	68
Co,Cr,Ni-TaC*	0.63	5	52	134	144	23	85
Co,Cr,Ni-TaC	2.54	2.5	50	122	151	33	98
Co,12Cr,12Ni	1.2	--	19	--	62	4	27
Co,10Ni-TaC	0.63	5	58	119	143	16	70

* Heat treatment -- 2 hrs. at 1340°C, W.Q., 48 hrs. at 750°C, A.C.

Table 7

Specific Impact Energy[64]
(joules/cm^2)

Alloy	Mini-Specimen	Standard Specimen
γ'/γ-Mo	156	N.A.
Ni,10Cr-TaC	46	N.A.
Co,15Cr-TaC	17	25
Co,15.7Cr,0.5Ni,3W-TaC	23	31
NiTaC-13	37	66
Rene' 80	N.A.	8

FIGURE CAPTIONS

Fig. 1. Transverse microstructures of several high temperature eutectic composites: a) γ/γ'-δ (0%Cr), R = 3 cm/hr b) γ/γ'-δ (6%Cr), R = 3 cm/hr c) Co,10Cr,10Ni-TaC, R = 2.5 cm/hr d) γ'/γ-Mo (AG-15) R = 1.9 cm/hr e) Ni-Ni_3Ta, R = 0.5 cm/hr f) Ni,10Cr,5Al-TaC, R = 0.6 cm/hr

Fig. 2. Effect of temperature on ultimate tensile strength of high temperature eutectic composites.

Fig. 3. Effect of interlamellar spacing, λ, on yield and tensile strengths of γ'-δ at 1093°C.[9]

Fig. 4. Effect of temperature and heat treatment on tensile properties of γ/γ'-δ (6%Cr).[12]

Fig. 5. Strength vs. temperature for γ'/γ-Mo (AG-15) grown at 2 cm/hr.[14]

Fig. 6. Comparison of transverse and longitudinal tensile strengths of several high temperature eutectic composites.[2]

Fig. 7. Temperature dependence of longitudinal and transverse strength and ductility of γ/γ'-δ (6%Cr).[17]

Fig. 8. Larson-Miller parameter curves for advanced turbine blade alloys and composites.[23]

Fig. 9. Larson-Miller parameter curves for stress-rupture of several eutectic composites, tested in argon (AG-15, AG-34 and Nitac 13),[14] vacuum (γ/γ'-δ),[14] or air (γ'-Ni_3Ta).[23]

Fig. 10. Effect of environment on Larson-Miller correlation for Nitac 13.[24]

Fig. 11. Effect of solidification rate (interfiber spacing or fiber radius) on creep-rupture properties at 980°C. a) rupture life and elongation of γ/γ'-δ (6%Cr)[28] b) minimum creep rate of γ/γ'-Cr_3C_2 vs. fiber radius, λ.[29]

Fig. 12. Longitudinal and transverse stress-rupture properties of γ'/γ-Mo (AG-15).[14]

Fig. 13. Comparison of specific 1000 hr. rupture strength of Cotac 33 (heat treated to precipitate carbides) with Cotac 3 and two nickel-base superalloys.[30]

Fig. 14. Effects of test temperature and precracking of fibers on high cycle fatigue resistance of Co,10Cr,10Ni-TaC.[31]

Fig. 15. High cycle fatigue of γ/γ'-δ, as affected by solidification rate, Cr content and precycling.[32,48]

Fig. 16. High cycle fatigue of Cotac in several microstructural conditions.[32,77]

Fig. 17. Ratio of σ_{max}/σ_{ys} vs. number of cycles to failure for Ni-45w%W in as-quenched and aged conditions.[33]

Fig. 18. Crack growth rate, da/dN, vs. stress intensity range, ΔK, for Cotac grown at 0.6 cm/hr. Data for maraging steel: ref. 90; γ-δ: ref. 36; γ/γ'-δ: ref. 38; 304SS: ref. 90.

Fig. 19. Influence of Cr content and temperature on crack growth rate of γ/γ'-δ.[38]

Fig. 20. SEM micrographs of stage I (crystallographic) cracking. a) longitudinal surface, Nitac, R = 0.6 cm/hr, $\Delta\sigma$ = 828 MN/m^2,[32] b) longitudinal surface, Cotac, R = 0.6 cm/hr, $\Delta\sigma$ = 830 MN/m^2,[78] c) fracture surface, Cotac, R = 0.6 cm/hr

Fig. 21. Fatigue striations in Nitac, solution treated after solidification, R = 0.6 cm/hr, $\Delta\sigma$ = 830 MN/m^2.

Fig. 22. Effect of prior temperature cycling in vacuum to 871°C on rupture life of four alloys in argon.[56]

Fig. 23. Charpy impact behavior of γ'-δ and γ/γ'-δ (6%Cr). Data for γ'-δ, MarM-200 and MarM-302 from ref. 79. Data for γ/γ'-δ from M. Gell. Curves appear in ref. 2.

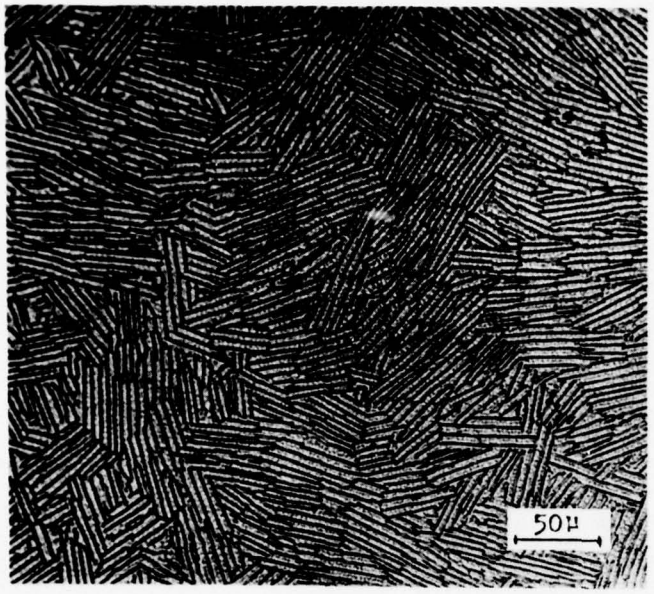

(a)

(b)

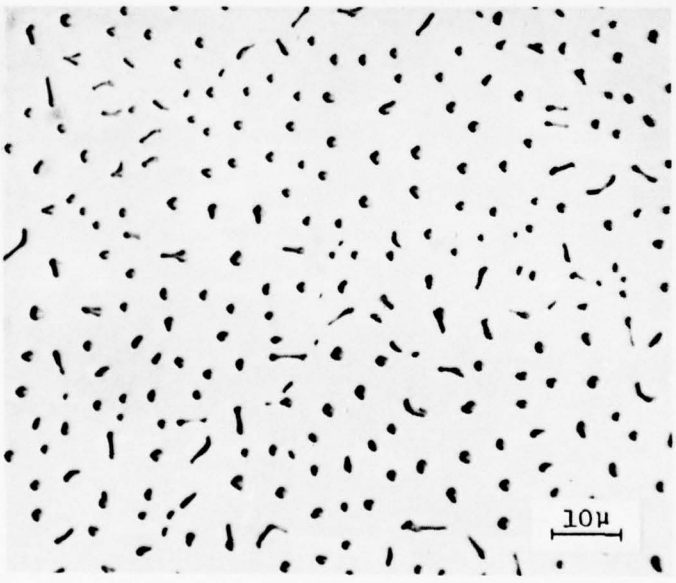

(c)

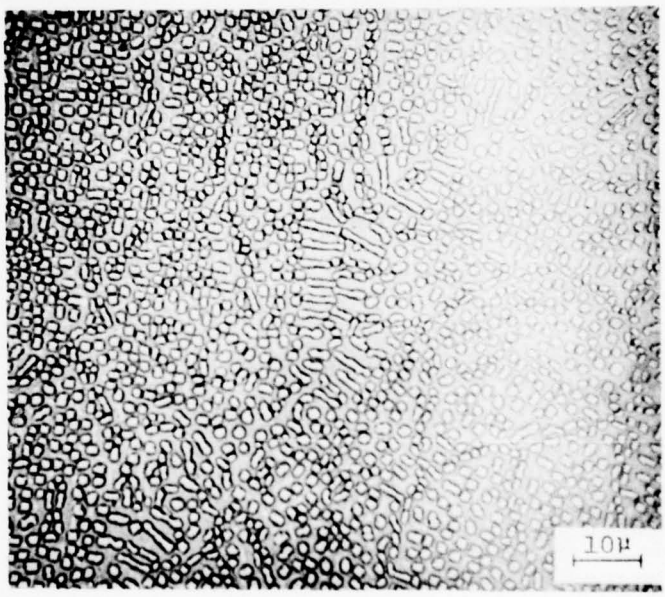

(d)

Fig. 1. Transverse microstructures of several high temperature eutectic composites: a) γ/γ'-δ (0%Cr), R = 3 cm/hr b) γ/γ'-δ (6%Cr), R = 3 cm/hr c) Co,10Cr,10Ni-TaC, R = 2.5 cm/hr d) γ'/γ-Mo (AG-15), R = 1.9 cm/hr e) Ni-Ni_3Ta, R = 0.5 cm/hr f) Ni,10Cr,5Al-TaC, R = 0.6 cm/hr

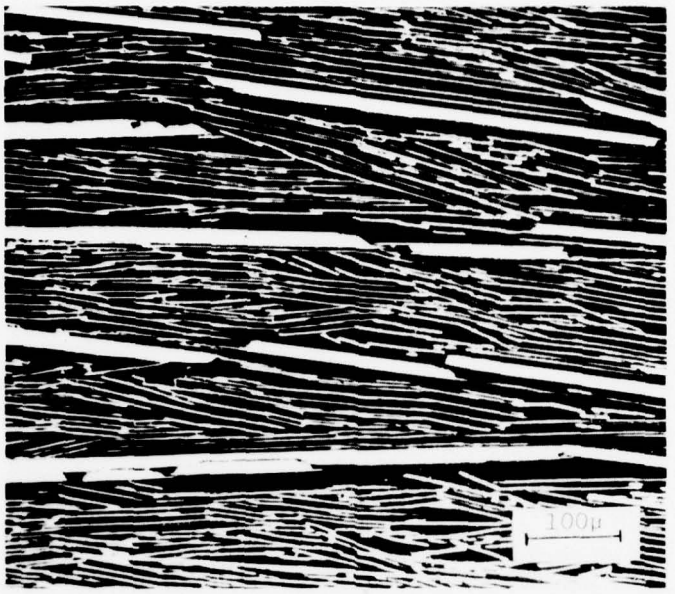

(e)

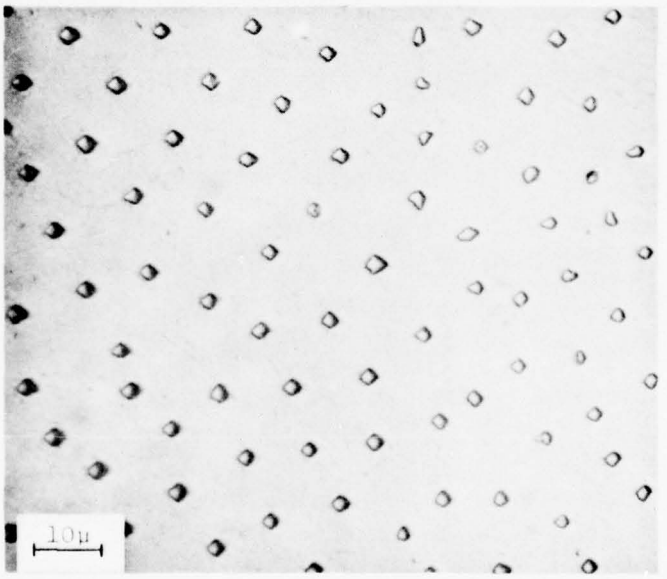

(f)

Fig. 1. Transverse microstructures of several high temperature eutectic composites: a) γ/γ'-δ (0%Cr), R = 3 cm/hr b) γ/γ'-δ (6%Cr), R = 3 cm/hr c) Co,10Cr,10Ni-TaC, R = 2.5 cm/hr d) γ'/γ-Mo (AG-15), R = 1.9 cm/hr e) Ni-Ni_3Ta, R = 0.5 cm/hr f) Ni,10Cr,5Al-TaC, R = 0.6 cm/hr

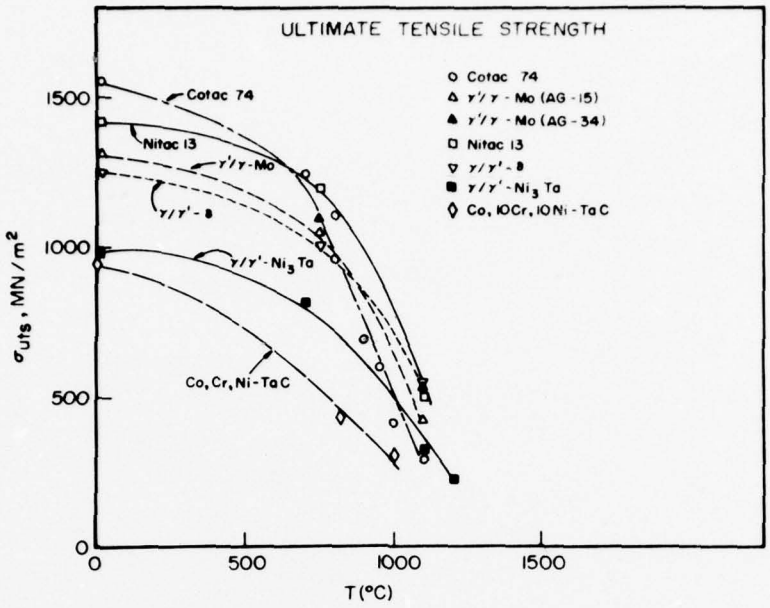

Fig. 2. Effect of temperature on ultimate tensile strength of high temperature eutectic composites.

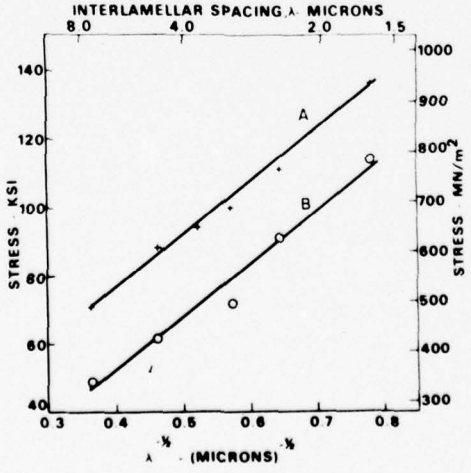

Fig. 3. Effect of interlamellar spacing, λ, on yield and tensile strengths of γ'-δ at 1093°C.[9]

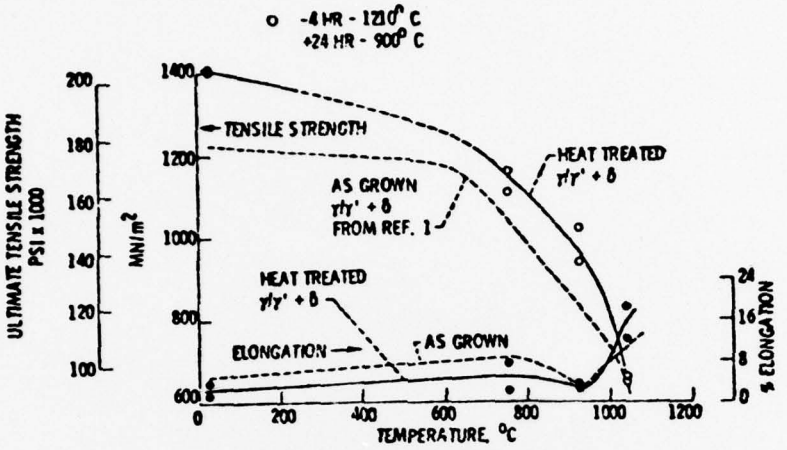

Fig. 4. Effect of temperature and heat treatment on tensile properties of $\gamma/\gamma'-\delta$ (6%Cr).[12]

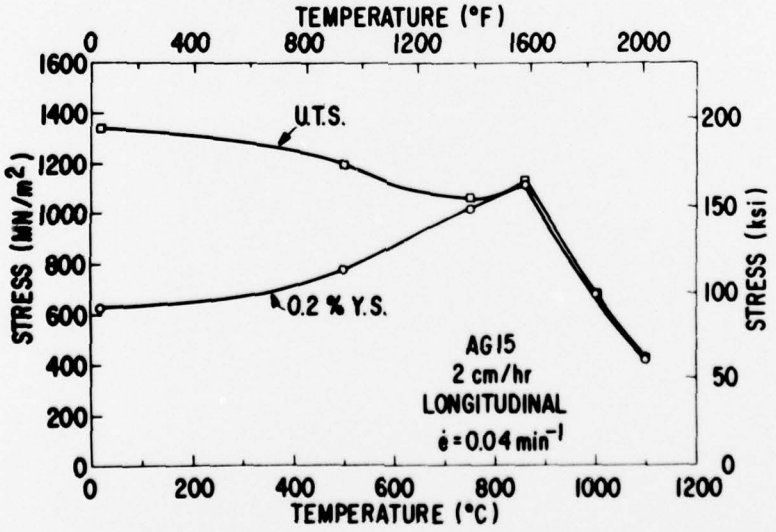

Fig. 5. Strength vs. temperature for γ'/γ-Mo (AG-15) grown at 2 cm/hr.[14]

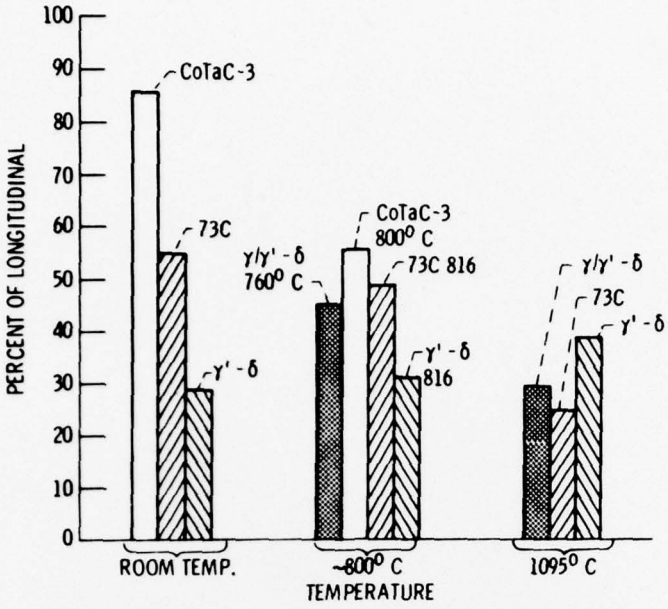

Fig. 6. Comparison of transverse and longitudinal tensile strengths of several high-temperature eutectic composites.[2]

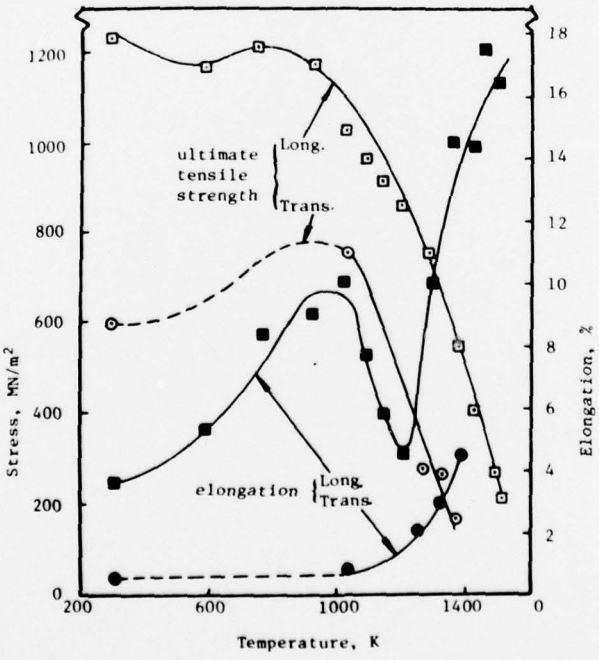

Fig. 7. Temperature dependence of longitudinal and transverse strength and ductility of γ/γ'-δ (6%Cr).[17]

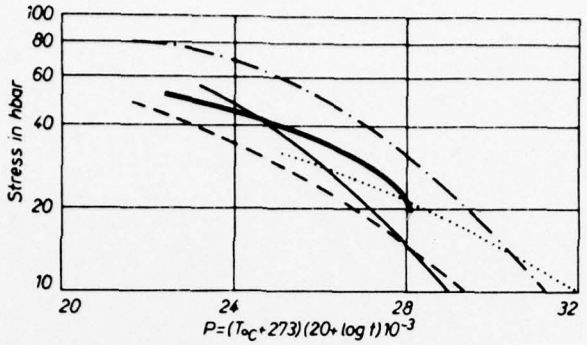

Figure 8. Larson-Miller parameter curves for advanced turbine blade alloys and composites.[23]

– · – · –Ni_3Al-Ni_3Nb 2 cm/h
. . . . . .COTAC-3 1–2 cm/h
————Ni_3Al-Ni_3Ta 1.33 cm/h
– – – –Ni-Ni_3Al-Ni_3Ta 1.33–120 cm/h
————IN-100 cast

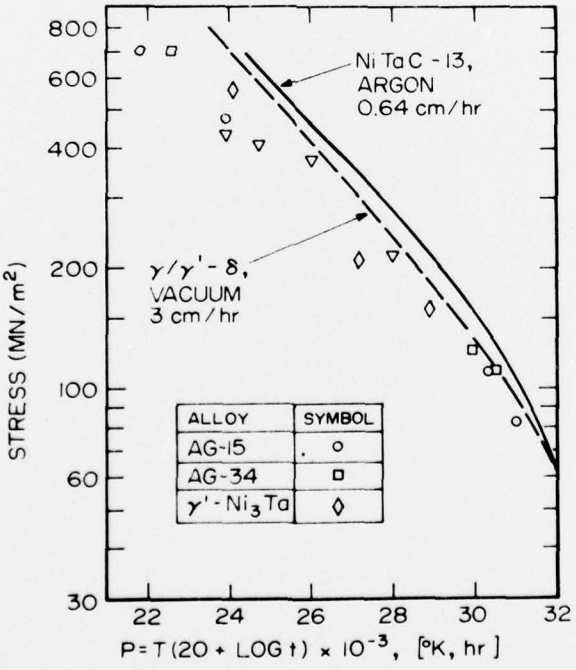

Fig. 9. Larson-Miller parameter curves for stress-rupture of several eutectic composites, tested in argon (Ag-15, AG-34 and Nitac 13),[14] vacuum (γ/γ'-δ),[14] or air (γ'-Ni_3Ta).[23]

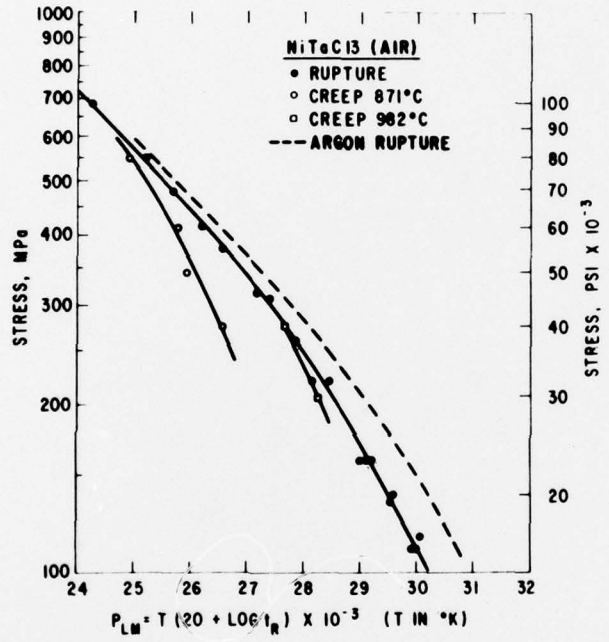

Fig. 10. Effect of environment on Larson-Miller correlation for Nitac 13.[24]

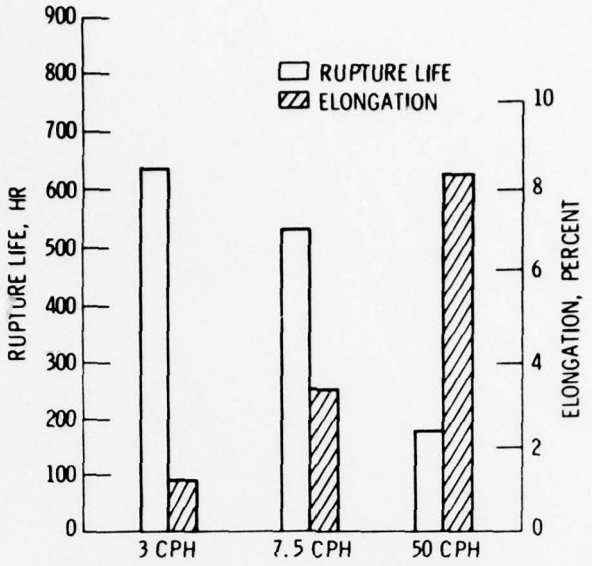

(a)

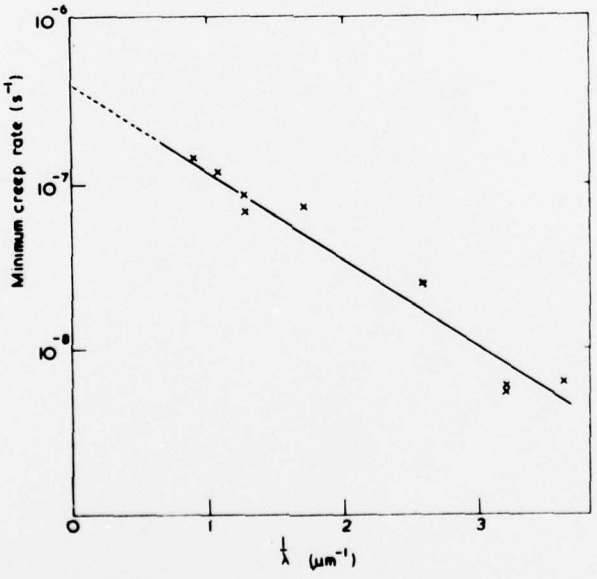

(b)

Fig. 11. Effect of solidification rate (interfiber spacing or fiber radius) on creep-rupture properties at 980°C. a) rupture life and elongation of γ/γ'-δ (6%Cr)[28] b) minimum creep rate of γ/γ'-Cr_3C_2 vs. fiber radius, λ.[29]

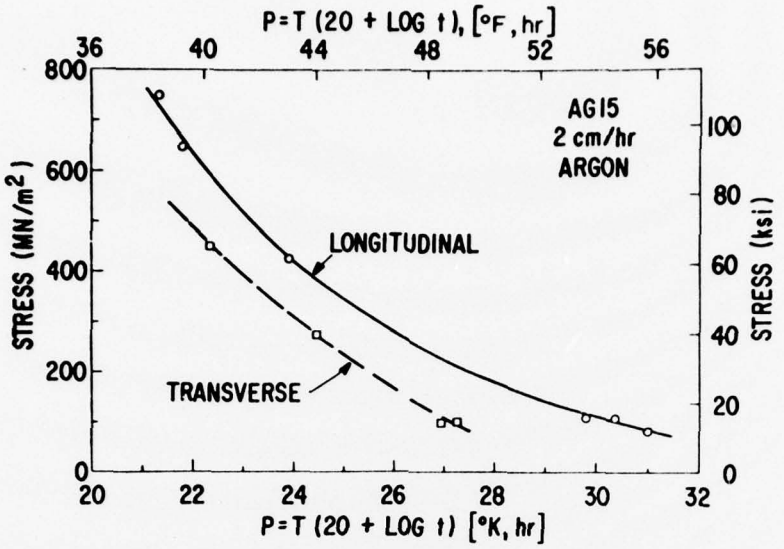

Fig. 12. Longitudinal and transverse stress-rupture properties of γ'/γ-Mo (AG-15).[14]

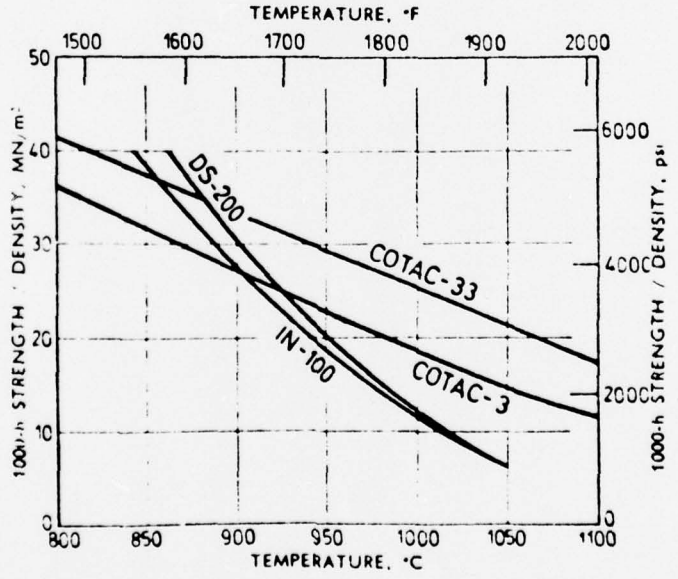

Fig. 13. Comparison of specific 1000 hr. rupture strength of Cotac 33 (heat treated to precipitate carbides) with Cotac 3 and two nickel-base superalloys.[30]

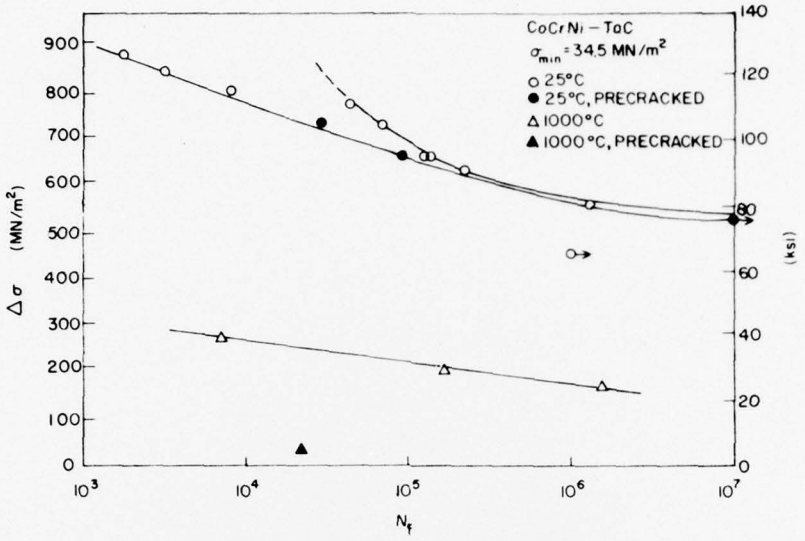

Fig. 14. Effects of test temperature and precracking of fibers on high cycle fatigue resistance of Co,10Cr,10Ni-TaC.[31]

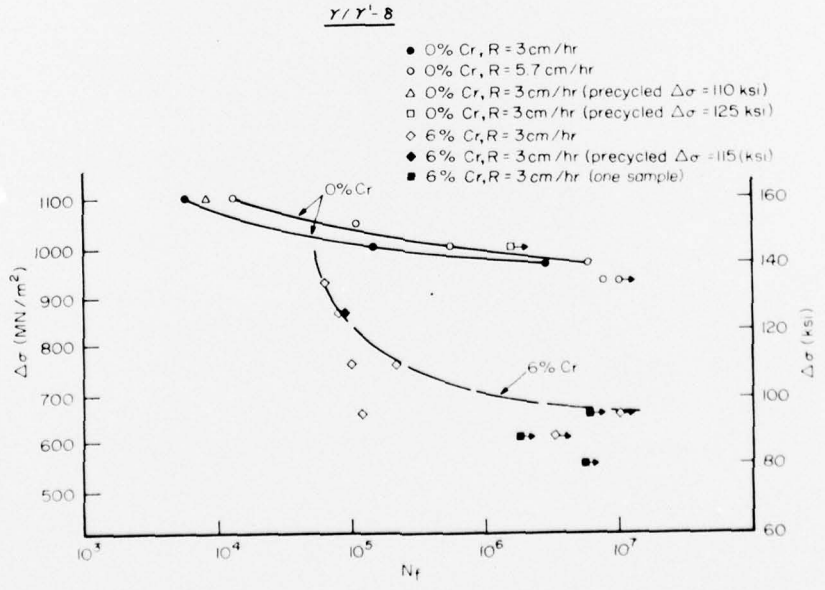

Fig. 15. High cycle fatigue of γ/γ'-δ, as affected by solidification rate, Cr content and precycling.[32,48]

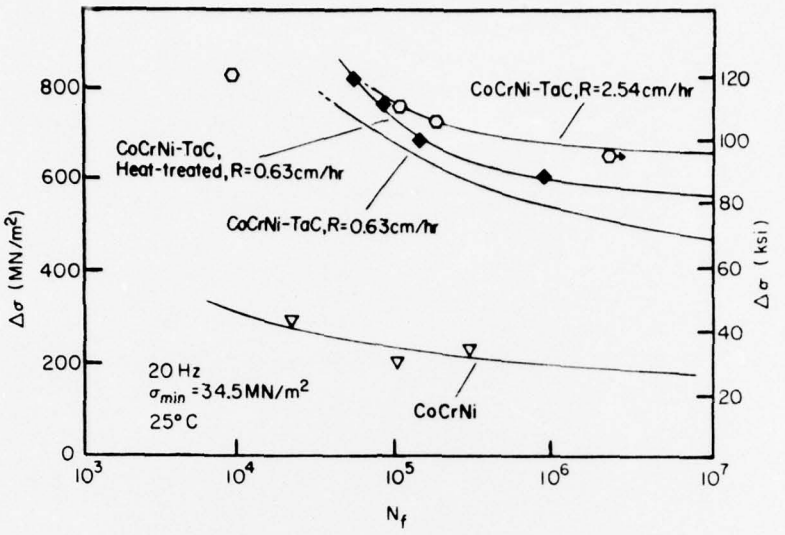

Fig. 16. High cycle fatigue of Cotac in several microstuctural conditions.[32,77]

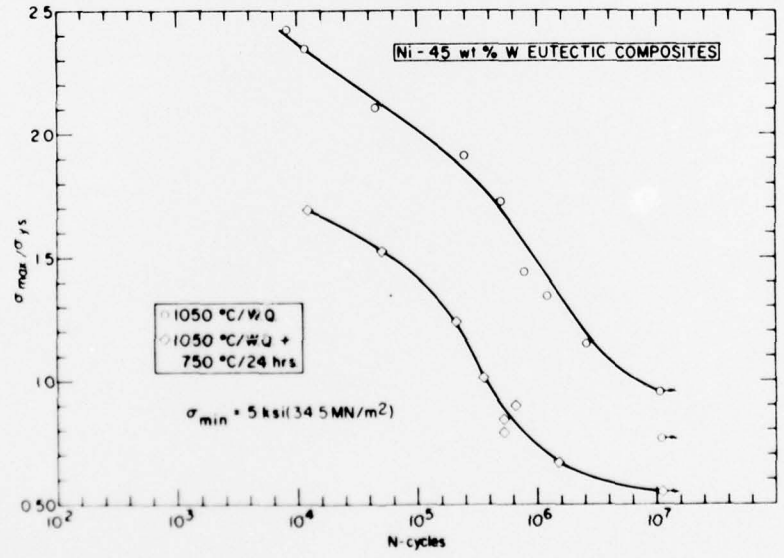

Fig. 17. Ratio of σ_{max}/σ_{ys} vs. number of cycles to failure for Ni-45w%W in as-quenched and aged conditions.[33]

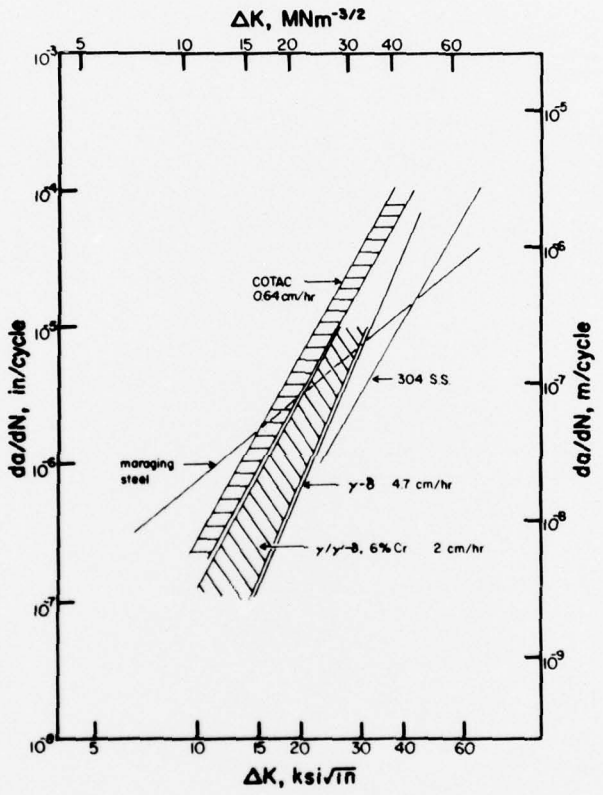

Fig. 18. Crack growth rate, da/dN, vs. stress intensity range, K, for Cotac grown at 0.6 cm/hr. Data for maraging steel: ref. 90; γ-δ: ref. 36; γ/γ'-δ : ref. 38; 304SS: ref. 90.

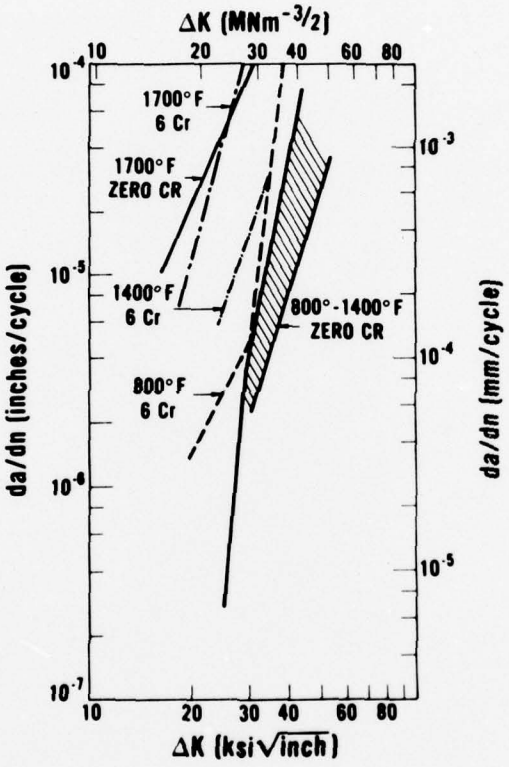

Fig. 19. Influence of Cr content and temperature on crack growth rate of γ/γ'-δ.[38]

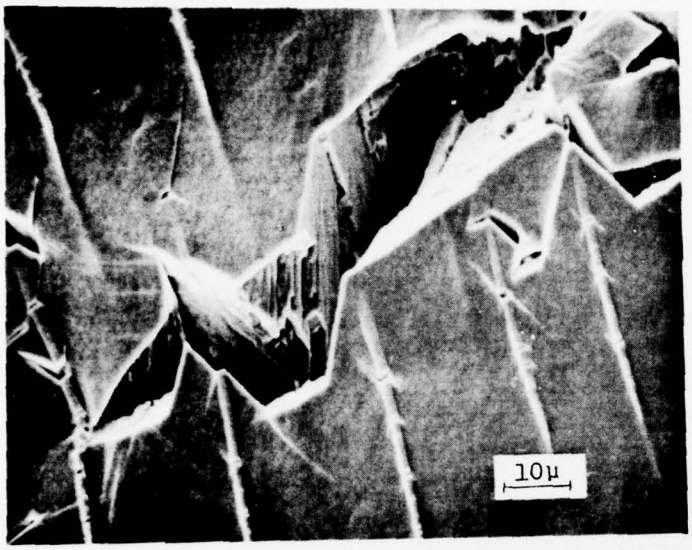

(a)

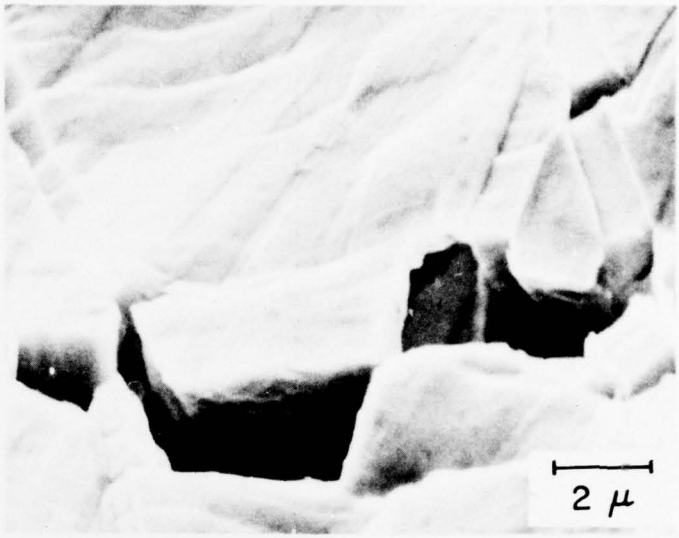

(b)

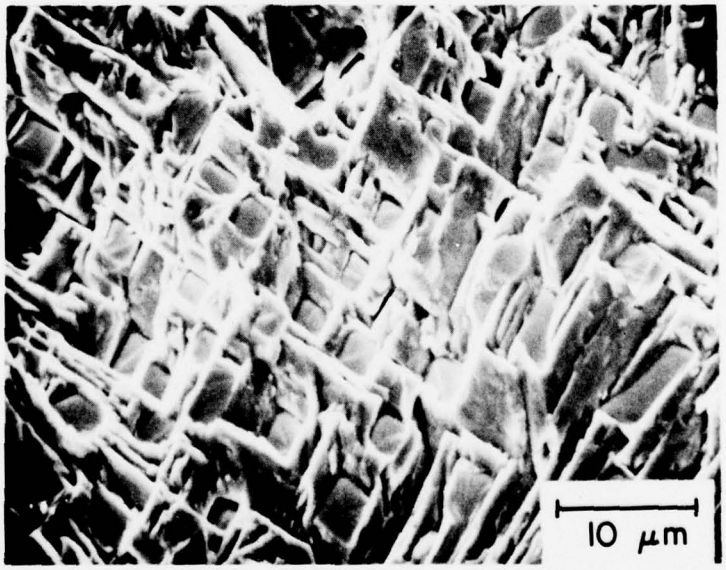

(c)

Fig. 20. SEM micrographs of stage I (crystallographic) cracking. a) longitudinal surface, Nitac, R = 0.6 cm/hr, $\Delta\sigma$ = 828 MN/m^2,32 b) longitudinal surface, Cotac, R = 0.6 cm/hr, $\Delta\sigma$ = 830 MN/m^2,78 c) fracture surface, Cotac, R = 0.6 cm/hr

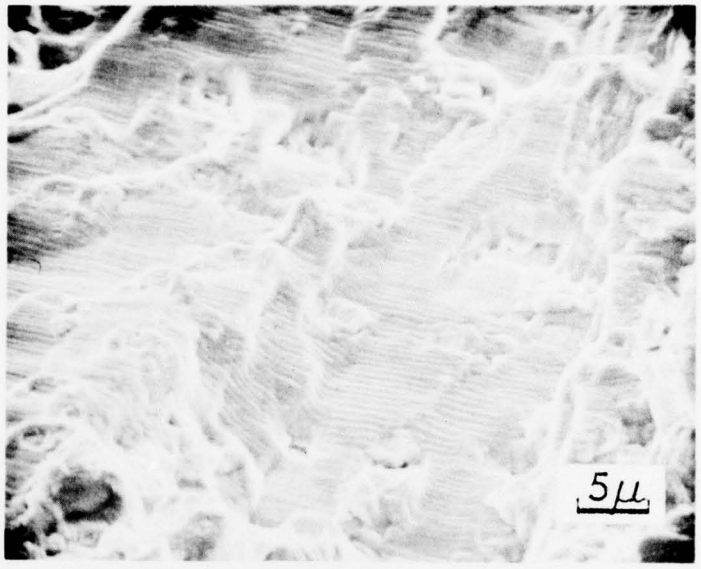

Fig. 21. Fatigue striations in Nitac, solution treated after solidification, R = 0.6 cm/hr, $\Delta\sigma$ = 830 MN/m^2.

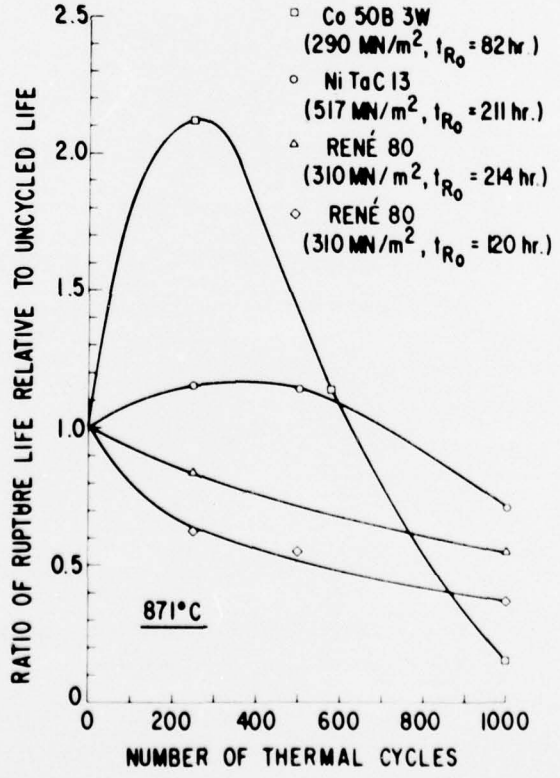

Fig. 22. Effect of prior temperature cycling in vacuum to 871°C on rupture life of four alloys in argon.[56]

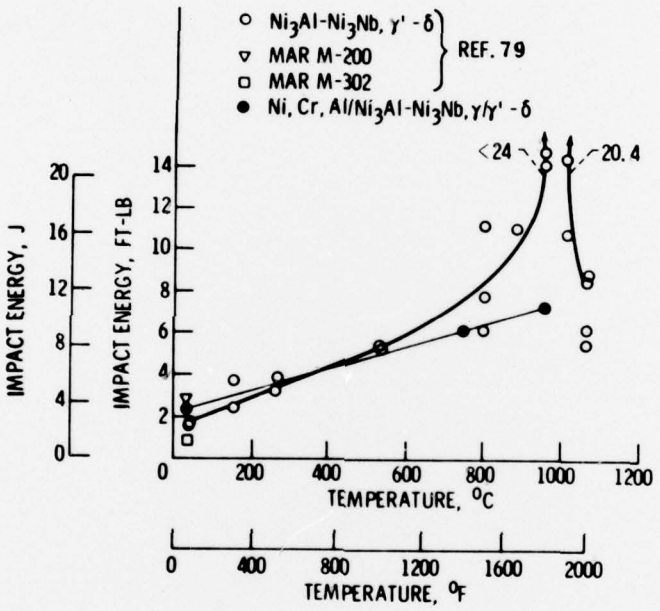

Fig. 23. Charpy impact behavior of γ'-δ and γ/γ'-δ (6%Cr). Data for γ'-δ, MarM-200 and MarM-302 from ref. 79. Data for γ/γ'-δ from M. Gell. Curves appear in ref. 2.

Unclassified

SECURITY CLASSIFICATION OF THIS PAGE (When Data Entered)

REPORT DOCUMENTATION PAGE

READ INSTRUCTIONS BEFORE COMPLETING FORM

1. REPORT NUMBER: Technical Report No. 3
2. GOVT ACCESSION NO.:
3. RECIPIENT'S CATALOG NUMBER:

4. TITLE (and Subtitle): High Temperature Eutectic Composites: Mechanical Behavior
5. TYPE OF REPORT & PERIOD COVERED: Technical Report
6. PERFORMING ORG. REPORT NUMBER:

7. AUTHOR(s): N. S. Stoloff
8. CONTRACT OR GRANT NUMBER(s): N00014-75-C-0503

9. PERFORMING ORGANIZATION NAME AND ADDRESS:
Materials Engineering Department
Rensselaer Polytechnic Institute
Troy, NY 12181

10. PROGRAM ELEMENT, PROJECT, TASK AREA & WORK UNIT NUMBERS: NR 031-745

11. CONTROLLING OFFICE NAME AND ADDRESS:
Office of Naval Research
Department of the Navy
Arlington, Virginia 22217

12. REPORT DATE: July 10, 1977
13. NUMBER OF PAGES: 61

14. MONITORING AGENCY NAME & ADDRESS (if different from Controlling Office):
Office of Naval Research Resident Representative
715 Broadway (5th Floor)
New York, NY 10003

15. SECURITY CLASS. (of this report): Unclassified
15a. DECLASSIFICATION/DOWNGRADING SCHEDULE:

16. DISTRIBUTION STATEMENT (of this Report)

Reproduction in whole or in part is permitted for any purposes of the United States Government.

DISTRIBUTION STATEMENT A
Approved for public release;
Distribution Unlimited

17. DISTRIBUTION STATEMENT (of the abstract entered in Block 20, if different from Report)

TR-3

18. SUPPLEMENTARY NOTES

19. KEY WORDS (Continue on reverse side if necessary and identify by block number)

Eutectic composites, creep, fatigue, impact, thermal cycling, fracture, tension, compression, gas turbines

20. ABSTRACT (Continue on reverse side if necessary and identify by block number)

The mechanical behavior of nickel and cobalt-base eutectic alloys is reviewed. Tensile compressive creep, impact and fatigue data are described and critically evaluated. Prospects for application of these alloys in gas turbines are described.

DD FORM 1 JAN 73 1473 EDITION OF 1 NOV 65 IS OBSOLETE
S/N 0102-LF-014-6601

Unclassified
SECURITY CLASSIFICATION OF THIS PAGE (When Data Entered)

302125